AN ABSTRACT OF THE THESIS OF

ROGER LEE PECK for the M. S. in Materials Science
(Name) (Degree) (Major)

Date thesis is presented October 12, 1965

Title AN INVESTIGATION INTO THE MECHANISMS OF ADHERENCE BETWEEN BOROSILICATE GLASS AND STEATITE CERAMIC AND BETWEEN BOROSILICATE GLASS AND ALUMINA CERAMIC

Abstract approved Redacted for Privacy
(Major professor)

A qualitative evaluation was made of the adherence between borosilicate glass and the ceramics, steatite and alumina. Three basic adherence studies were performed.

(1) A comparison between the x-ray diffraction patterns of the ceramic and the fused glass-ceramic powder mixture was made to determine if any new compounds were formed at 1200° C.

(2) A metallographic examination of the interfacial region of actual seals made at 800°, 900°, 1000°, 1100°, and 1200° C was made to observe the transition zone and any new phases formed.

(3) A hydrostatic rupture test and a metallographic and stereoscopic examination of the resulting fracture surfaces were made in order to get a qualitative evaluation of the adherence developed in seals formed at various temperatures.

The results of each investigation indicated that good glass-ceramic adherence was achieved. The x-ray diffraction work suggested that new compounds were formed at both glass-ceramic interfaces. In the alumina system, the resulting diffraction pattern closely resembled both an aluminum borate and an aluminum silicate. In the steatite system, a close match was not made, but the new pattern did resemble magnesium meta silicate.

The metallographic work revealed that, in the steatite system, extensive interdiffusion of the glass and ceramic phases occurred. Devitrivication was observed in seals made at 1200° C, and cracks appeared when these seals were cooled. Neither phase in the alumina system was so obviously affected by high temperatures. A few small crystals were found on the ceramic at the interface, and glass filled some of the ceramic voids near the interface, but evidence of extensive diffusion was not observed.

The hydrostatic rupture test data showed that the strength of the alumina seals improved with temperature. Similar data were not collected for the steatite seals, for too many samples broke improperly. Examination of the fracture surfaces in both systems indicated that the crack generally propagated through the glass phase. This suggests that the solid-liquid interfacial energy is somewhat smaller than the solid-gas interfacial energy, or the energy of adherence is large.

AN INVESTIGATION INTO THE MECHANISMS OF ADHERENCE BETWEEN BOROSILICATE GLASS AND STEATITE CERAMIC AND BETWEEN BOROSILICATE GLASS AND ALUMINA CERAMIC

by

ROGER LEE PECK

A THESIS

submitted to

OREGON STATE UNIVERSITY

in partial fulfillment of
the requirements for the
degree of

MASTER OF SCIENCE

June 1966

APPROVED:

Redacted for Privacy

Associate Professor of Mechanical Engineering
In Charge of Major

Redacted for Privacy

Head of Department of Mechanical and Industrial Engineering

Redacted for Privacy

Dean of Graduate School

Date thesis is presented October 12, 1965

Typed by Opal Grossnicklaus

ACKNOWLEDGMENTS

The author considers it a distinct pleasure to have worked with Dr. Welty during the past year. His keen sense of experimental direction saved many hours of what would otherwise have been wasted time. Jack Kellogg and Ed Riesland machined the magnetic mortar and pestle and the hydrostatic tensile test components. The technical assistance of Dan Carstea, who took enough time out of his full schedule to make the four diffractometer plots, is gratefully acknowledged. The author's wife, Bonnie Jean Peck, spent many hours deciphering the first rough draft and typing it into a more workable form.

Finally, appreciation is expressed to Bell Telephone Laboratories whose generous financial support made this interesting project possible.

TABLE OF CONTENTS

TABLE OF CONTENTS (Continued)

LIST OF FIGURES

LIST OF FIGURES (Continued)

Figure

LIST OF FIGURES (Continued)

LIST OF TABLES

AN INVESTIGATION INTO THE MECHANISMS OF ADHERENCE BETWEEN BOROSILICATE GLASS AND STEATITE CERAMIC AND BETWEEN BOROSILICATE GLASS AND ALUMINA CERAMIC

I. INTRODUCTION

With the birth of the electronics industry, considerable attention was directed toward glass and its potential role in the construction of electron tubes. Some time later, ceramics, too, were found to possess properties useful to the industry. More recently, these two materials have found complimentary uses in the construction of semiconductor devices.

Uses of Glass in Electronics

The most common uses of glass in the construction of electron tubes are as an electrical insulator between metallic electrodes, as a gas envelope, and as a mechanical support (5). After the discovery of semiconductor devices, it was thought at first that gas-tight enclosures would no longer be required, but experience proved that the life of these solid state devices was impaired by exposure to the atmosphere. Thus, enclosure designs resembling those of electron tubes are found today on transistors (5).

Uses of Ceramics in Electronics

A variety of outstanding properties of ceramics has allowed

them to replace glass at several points in the construction of electron tubes and semiconductor devices. Perhaps their most useful properties are low electrical and thermal conductivities at high temperatures (4). Although both glass and ceramic can be effectively sealed to conductor metal leads, the relative ease with which the glass-metal seal can be made causes it to be more commonly used.

Area of Project Application

The study of glass-to-ceramic adherence is especially applicable to enclosure techniques where a component or small circuit is encased in a ceramic shell and sealed with glass. The ceramic shell provides protection from a hostile environment, and the glass allows a tight seal for the electrical leads. Simultaneous use of the advantageous properties of glass and ceramics necessitates the bonding between them. This project is directed toward the understanding of the mechanism of their adherence.

II. BACKGROUND

A general background in the structure and properties of glasses and ceramics is presented in an effort to give more meaning to the specific properties of the materials used in this research. The phenomenon of adherence is examined, experimental methods for evaluating adherence are enumerated, and the scope of this paper is thereby defined.

Structure and Properties of Glass

A better understanding of the properties and behavior of glass is possible if one is first familiar with the fundamentals of its solid state.

Structure of Glass

Most oxides crystallize when cooled from the liquid state. There are several important exceptions that prefer instead to form a rigid, noncrystalline condition. Zachariasen (30) in 1932, in a classic study of atomic arrangements in glass, was able to develop a model that provided satisfactory answers to why some oxides were crystalline and others were glassy. Using x-ray techniques, he observed that the basic unit in both the glassy and crystalline forms of silica was the silicon atom tetragonally coordinated by oxygen

atoms, and that interatomic distances in both forms were almost identical. He postulated that the main differences between the two states were that in glass, the silica unit was repeated in a three-dimensional random network while in the crystal, it was repeated in a three-dimensional periodic lattice.

Zachariasen postulated that, in order for an oxide, M_xO_y, to be able to form a random network, it must satisfy the following conditions (30):

(1) 0 atom can link with no more than two M atoms

(2) Coordination number of 0 ions about M is small, less than four

(3) Polyhedra share corners only

(4) At least three corners shared

By manipulating Si-0 tetrahedra, it can be shown that only the following oxides can form the required network:

M_2O_3, if oxygen is in triangular coordination around M

MO_2 and M_2O_5, if oxygen is in tetrangular coordination around M

Neither M_2O nor MO satisfy all the postulates.

Oxides, then can be classified according to their ability to either form or modify the network.

Network formers: Principally SiO_2, B_2O_3, and P_2O_5

Network modifiers: Alkali and Alkaline Earth oxides such as

K_2O, Na_2O, MgO, BaO, and CaO

Intermediates: Al_2O_3

The modifier oxides, as seen by their formulae, cannot form the network by themselves, but their addition to an established network greatly modifies the resulting properties. Intermediates are also unable to form the network but can substitute for the network former to maintain the network (11).

Zachariasen's model explains which oxides can form the glassy state. Uncommonly high viscosity at the equilibrium melting point is the reason why the glassy state actually does form. In a normal manufacturing process, the atomic rearrangements necessary for the phase change from a liquid to a crystalline solid do not take place because of excessive viscosity (7).

Modifiers and Intermediates. When a modifier oxide is added to a silica network, the O/Si ratio is increased, and some oxygen atoms can make only one bond with Si. The remaining bond is made loosely with the modifier cation which is easily accommodated interstitially. As seen in Figure 1, the oxygen atom now is nonbridging, and the network is disrupted (16, 26). An increase in the coefficient of thermal expansion and a lowering of the melting point are resulting changes in physical properties.

Figure 2 shows how an intermediate oxide, Al_2O_3, can replace silica in the network. Since Al has plus three valence, electrical neutraility is maintained by the plus one charge contributed by an interstitial atom (2). In most glasses, the gram-mole ratio of Al_2O_3/modifier oxides is close to one (18).

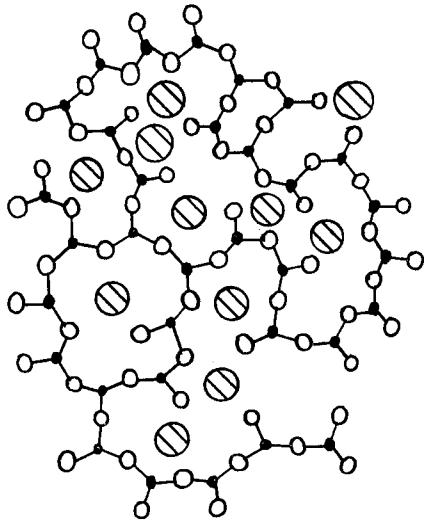

• Si O O Na

Figure 1. Two-dimensional silica network modified by sodium (28).

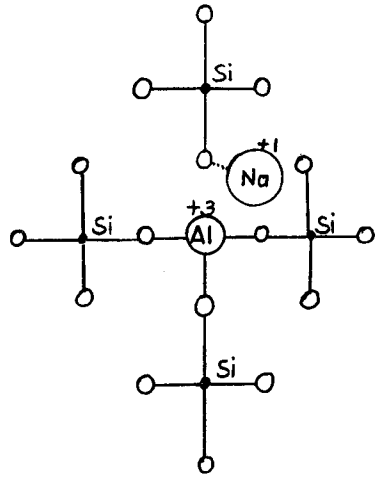

Figure 2. Silicon in glass network replaced by aluminum. Sodium ion required for electroneutrality (2).

Stability of Glass. There are two reasons why a supercooled liquid like glass fails to crystallize upon cooling. Either the nucleation rate is too small, or the grain growth is too slow. Heterogeneous nucleation is not likely because glass is an excellent solvent for "dirt". Homogeneous nucleation is unlikely because of the high activation energy for diffusion across the liquid-solid boundary. Even if nucleation were able to take place, grain growth would be negligible because of slow diffusion rates in the highly viscous liquid phase (8, 18, 19).

Devitrification. Devitrification, or crystallization, occurs either in a controlled manner as the result of a carefully programmed heat treatment or in an uncontrolled manner as the result of local changes in composition. Controlled devitrification is the basis for the new technology of glass-ceramics (18). Nucleation is

accomplished either by causing special metal ions to nucleate as metal particles or by developing a condition of two-phase separation of tiny emulsion droplets and homogeneously nucleating these droplets. In either case, a heterogeneous nucleus is provided on which the remainder of the glassy matrix can grow. The growth rate is increased with higher temperatures. By selecting a nucleation material with a crystal system and lattice parameters similar to those of glass, a condition of nearly complete devitrification can be accomplished (18).

Properties of Glass

The physical properties of glass can be quite easily related to its solid state.

Viscosity. In liquids, the relative movement of atoms is restricted by attractive forces between neighbors. "High viscosities in silicate systems result from the presence of variable size and shape large silicate ions and chains which restrict flow under a shearing stress"(14).

Coefficient of Thermal Expansion. In the lower temperature range, the graph of temperature versus length of a typical glass displays a shallow positive slope below about 400° C and a rapidly increasing slope above about 500° C. Slowly increasing bond distances with increasing energy account for the low temperature behavior,

and network dilation causes the steep slope above 500° C (2, 8, 26). Modifier oxides disrupt the silica network and cause it to be more loosely bound together. A given amount of heat energy has fewer bonds to stretch, and the coefficient is increased.

As stated earlier, B_2O_3 forms a planar network with oxygen triangularly coordinated around boron. The addition of silica causes some of the boron atoms to form tetragonal bonds, and the network is thereby bound together more tightly (26). A given amount of heat energy finds more bonds to stretch, and hence the coefficient of expansion for borosilicate glasses is generally less than that for other glasses.

Transparency. A simplified explanation for the transparency of glass is provided by the band model (2). Any quanta of light in the visible spectrum have insufficient energy to excite electrons from the valence band. They pass right through and are not absorbed.

Color. Color results from the absorption of radiation in the visible spectrum. Electronic transitions in the atoms present in glass provide the correct quantum jumps, but absorption can occur only when unfilled energy levels are available. The transition metal atoms present provide these unfilled levels. Commercial colors are prepared by putting the metal oxides in solution, by suspending them as colloidal particles, or by crystallizing them as tiny crystals (14,

21, 26).

Electrical Conductivity. Electricity is conducted by the diffusion of the modifier-oxide cations; the tightly bound network contributes relatively nothing. As would be expected, conductivity is enhanced by smaller cations, higher temperatures where the network is dilated, and smaller charges on the cations (2, 8, 26).

Physical Strength. The strength of glass is not a basic characteristic of the solid state. It is, rather, a function of surface condition, size and shape of the test specimen, and rate of loading (9). The effect of these outside parameters is that ultimate strength data is meaningful only when a large number of identical specimens are tested. There is a large variance between samples, and Shand feels that it is desirable to average the results from 20-30 tests to get one reliable data point (26).

Brittleness. The plastic yielding of materials is usually attributed to the movement of dislocations. In the random structure of glass, dislocation theory has no meaning. Glass is brittle because of a lack of ability of atoms to rearrange themselves on a large scale (9).

Fracture. Glass is about one-tenth as strong in tension as in compression. All failures are, therefore, in tension (26). The study of a fracture surface will reveal some important information concerning the initiation and propagation of fracture. The origin of

fracture is normally at a surface defect and is surrounded by a small, smooth plane. The stress orientation is normal to this plane. Faint, concentric ridges, or Waller lines, contain the defect and plane, and the propagation direction is normal to these lines. Further away from the defect is a region of shattered glass where propagation speed is excessive (5, 26).

Structure and Properties of Ceramic

Such a wide variety of materials is included within the classification of ceramics that the study of general structure and properties is almost too broad to have useful meaning.

Structure of Ceramic

Ceramics are a mixture of crystalline materials held together by a glassy binder (14). Commercially available ceramics include mixtures of a wide range of compositions, proportions, and arrangements. This diversification can readily be seen in Table I which is a condensation of a table presented by Salmang (25).

Properties of Ceramic

Considering again Table I, it can be seen that the properties of ceramics are not consistent. Properties are most successfully related to structure by considering a weighted average of the specific

components. Therefore, alumina ceramic is strong because its major constituent, Al_2O_3, is strong, and steatite is considerably weaker because its major constituent, a mineral closely related to talc, is weak.

Table I. Classification of ceramic products.

A. Clay Wares (body porous and opaque)	
Constructional	Domestic
Bricks	Flower Pots
Refractories	White earthenware pipe-clay ware

B. Sintered Material			
Stoneware		Porcelain	
(vitrified with translucent edges)		(translucent)	
Constructional	Domestic	Constructional	Domestic
Flagstone	Wedgewood ware	Electrical porcelain	Bone china

C. Electro-technical Porcelain and Super-refractories
Steatite, Al_2O_3, and other pure metal oxides

Materials

The materials used in this research project were 7052 borosilicate glass made by Corning Glass Company, F66 steatite ceramic made by Western Electric, and alumina ceramic made by American Lava Corporation. A brief description of their specific properties

and more common uses is presented. The wet chemical analyses were made by Emhart Corporation which specializes in testing of glass and ceramic materials.

Borosilicate Glass

Borosilicate glasses are characterized by a low coefficient of thermal expansion, 46 10^{-7}/° C, a high softening point, 708°C, and a good corrosion and thermal shock resistance (16, 26). This combination of properties allows borosilicate glasses to be used for glass-to-metal electrical seals, laboratory glassware, and household cooking ware. The Corning specifications and results of the wet chemical analysis are tabulated in Table II.

Table II. Comparison of specifications and wet analysis of 7052 glass.

Constituent	Specification wt. percent	Analysis wt. percent
Silicon dioxide	64.5	64.62
Iron plus aluminum oxide	7.5	7.60
Barium oxide	3.0	2.92
Potassium oxide	3.0	3.45
Sodium oxide	2.0	1.75
Boric oxide	18.5	18.32
Lithium oxide	0.5	0.89
Calcium and magnesium oxide	0.1	Not analyzed
Chlorides and fluorides	0.5	Not analyzed
		99.55 Total

F66 Steatite

Steatite, in either its natural state or manufactured state, is a relatively weak ceramic (10,000 psi) with a coefficient of expansion of about $75 \times 10^{-7}/°C$, a softening point of 1240° C, and a high resistance to electrical current (25). It is machinable in its unfired state. Uses include high temperature vacuum tube insulators, electronic parts requiring low dielectric losses, and insulating sleeves for electrical leads on furnaces (3). Western Electric specifications and the results of the wet chemical analysis are tabulated in Table III.

Table III. Comparison of specifications and wet chemical analysis of F66 ceramic.

Constituent	Specification wt. percent	Analysis wt. percent
Silicon dioxide	49.0 ± 2.5	50.38
Iron plus aluminum oxides	9.2 ± 1.0	7.38
Barium oxide	15.7 ± 1.0	15.37
Magnesium oxide	26.2 ± 1.0	26.14
Iron oxide	<1.0	0.56
Calcium oxide	<0.75	Not analyzed
Total alkali oxides	<0.2	"
Chlorides	<0.01	"
Sulfur	<0.001	"
		99.83 Total

Alumina

The most significant properties of alumina include its low electrical conductance at elevated temperatures, its high strength (25, 000 psi), its high maximum useful temperature of 1900° C, and its chemical stability at high temperatures. Its coefficient of expansion is about $80 \times 10^{-7}/°$ C. The excellent high temperature properties of alumina and its commercial availability make it a useful laboratory material (14). Its most common uses are as electrical resistance furnace cores and crucibles for molten metal (3). Table IV shows the results of the chemical analysis obtained for the alumina ceramic used in this work.

Table IV. The composition of alumina ceramic produced by American Lava Corp.

Constituent	Analysis wt. percent
Silicon dioxide	5. 22
Iron plus aluminum oxides	94. 64
Barium oxide	0. 00
Magnesium oxide	0. 00
	Total 99. 86

Theory of Adherence

The tendency for two surfaces to adhere when placed in contact is a function of certain chemical and physical surface phenomena which are, in turn, related to cohesive forces at the interior of the substances (18). These interior cohesive forces are the familiar bonding forces, ionic, covalent, metallic, and van der Waals. Many substances appear to have a combination of types of bonding. Ceramic and glass are materials which cannot be classified as having purely one type of bonding.

Catastrophically forming a new plane surface through a material decreases the coordination number of the surface atoms and thereby reduces their screening effectiveness. The resultant increase in energy at each surface is called surface energy (14, 20, 26). The measured surface energy is somewhat less, however, because of the tendency for the surface atoms to screen each other. For a liquid, this tendency manifests itself as a force which diminishes the amount of surface area; this is called surface tension. The surface energy of a solid surface can be reduced by the adsorption of foreign atoms (12, 20).

Two phases will form an interfacial bond if the energy of the resultant system is lower than the sum of the energies of the original phases. For a liquid and solid,

$$\Delta F = F_{sl} - (F_{sg} + F_{lg}) \tag{1}$$

where ΔF is the change in energy resulting from the formation of the solid-liquid system, F is the surface energy defined by the subscripts, and s, l, and g are solid, liquid, and gas, respectively.

Adhesion between two materials can be defined as the energy necessary to pull them apart cleanly (14, 25). The increased energy caused by the structural discontinuity, or mismatch, at the interface reduces the necessary work of separation. If one of the materials is in the liquid state, the energy of adhesion can be represented by the Dupre equation.

$$F_{ad} = F_{sg} + F_{lg} - F_{sl} \tag{2}$$

The strongest bond would be one with the lowest interfacial energy F_{sl} (14, 15, 20). When both materials are able to take up strain and have different coefficients of expansion, less work is required, and a strain term is added.

$$F_{ad} = F_{sg} + F_{lg} - F_{sl} - F_{strain} \tag{3}$$

Experience in the mechanical testing of glass-to-metal seals indicates that if F_{sl} is considerably smaller than F_{sg} and the expansion coefficient is small, fracture occurs in the glass phase rather than at the interface. If the coefficient is large and/or F_{sl} is nearly equal to F_{sg}, the seal tends to separate at the interface (20).

Glass-to-Metal and Ceramic-to-Metal Seals

Before commencing the study of glass-to-ceramic seals, it is instructive to study glass- and ceramic-to-metal seals. These seals, especially glass-to-metal, have received considerable attention in the development of electronics technology. In both cases the strong adherence is found to depend on a good chemical bond across the interface.

Glass-to-Metal Seals

Pask and his co-workers, in a study extending over several years, wrote eight papers under the general title of "Fundamentals of Glass-to-Metal Bonding". The eighth paper summarizes the conclusions they reached. It was found that a carefully controlled metal-oxide layer reacted with the molten glass to form a transition layer. Silicon atoms in molten glass attempt to lower their internal energy by screening themselves with 0 atoms. Thus, a driving force for the solution of the metal oxide layer by the glass is developed. If this layer is not completely dissolved, it will remain covalently bound to the metal. At the same time, some of the 0 atoms will interpenetrate the layer of 0 screening atoms on the glass surface and provide additional screening for the Si atoms. Thus, the condition of the metal oxide layer plays a major role in establishing

the transition layer. A strong chemical bond is maintained across this layer (20).

Ceramic-to-Metal Seals

Less attention has been directed toward understanding the mechanisms of ceramic-to-metal seals. However, the fundamental of gaining good adherence by establishing a chemical bond across the interface is generally undisputed (4). Pulfrich (24), in an early work, felt that a good seal could be formed if the ceramic were first coated with an extremely fine-particled refractory metal powder. Sintering caused a eutectic binder of the ceramic to flow into the porous metal layer. Cooling caused the binder to crystallize and mechanically lock the coated layer. Normal soldering methods could then be used in attaching a piece of metal to this locked-on layer.

Cole (6) postulated that the glassy phase of the ceramic migrated into the porous metal layer and reacted with oxides there in a manner similar to the one mentioned for the glass-to-metal bond. Pincus (22) considers the following conditions as features of all good ceramic-to-metal seals:

1. Controlled oxidation of the metal.
2. Chemical reaction between the metal oxide and the ceramic to form an interfacial zone.
3. Bonding between the metal and ceramic through the

interface is a graded, continuously coherent structure compatible with the ceramic.

Apparently, much work remains to be done before the mechanism of ceramic-to-metal adherence is well understood.

Evaluation of Adherence

General techniques for evaluating adherence include contact-angle measurement and mechanical testing. Contact-angle work makes use of the balance of forces that exists at the point of gas-liquid-solid contact. Basically, the spreading of a liquid over a solid surface indicates that the solid-liquid interface represents a system of lower surface energy than the sum of the surface energies of the two phases separated. Good adherence is indicated by an angle at the interior of the drop of 25° or less (20).

Mechanical testing of a seal and an examination of the resulting fracture surface can give quantitative measurements of strength of the specific seal design.

Since the formation of a chemically bonded transition zone is so important, other techniques, including x-ray diffraction, metallographic, and electron microprobe, may be applied in an attempt to identify any new phases and to delineate the zone of reaction.

III. EXPERIMENTAL PROCEDURES

Three of the basic adherence studies mentioned earlier were carried out on the glass-ceramic interface material: (1) an x-ray diffraction examination of powdered samples of the interface, (2) a metallographic examination of a section through the interface, (3) a tensile strength evaluation of the quality of the bond, and an examination of the fracture surface of the failed tensile specimen.

X-Ray Examination

Powder samples of likely interfacial materials were examined by diffraction techniques using both the Debye camera and the diffractometer. Attempts to identify the resulting patterns were made using the comparative methods afforded by the Index to Powder Pattern Diffraction File (27).

Sample Preparation

Samples of the 7052 glass, F66, and Al_2O_3 were prepared in the powder form by being crushed in a carburized magnetic mortar and then passed through a 325 mesh (44 micron) screen. Cleanliness was achieved by cleaning the mortar, pestle, and screen ultrasonically and then rubbing a small magnet back and forth through the powder.

Samples of material likely to be found at the glass-ceramic interface were made by mixing 1:1 by weight portions of 7052/F66 and 7052/Al_2O_3 powders. These mixtures were initially fused at 1000° C for 25 hours, furnace cooled, repowdered, and recleaned with the magnet. Specimens suitable for x-ray powder pattern diffraction examination using the Debye camera were made by binding the powder with duco cement diluted with acetone and then rolling the mixture into small rods measuring approximately 0.5 mm × 8 mm.

Subsequent metallographic work showed evidence of some higher temperature reactions in the F66-glass seal. Therefore, a 1:1 mixture of glass and F66 was fused at 1200° C for 25 hours and prepared for the Debye camera in the same way.

Debye Camera Photographs

Norelco x-ray equipment was used. In an effort to obtain an optimum line distribution and line intensity, a variety of target materials and exposure times was tried. Best results were obtained using the following parameters.

Table V. X-ray powder-pattern exposure parameters.

Sample	KV	MA	Target	Filter	Exposure time, hr.
F66	30	8	Cr	V	12.2
F66/glass	30	8	Cr	V	10.2
Al_2O_3	35	8	Fe	Mn	3.3
Al_2O_3/glass	35	8	Fe	Mn	4.2

No-screen film was used, and all pictures were developed for five minutes in Kodak Rapid X-Ray Developer and fixed for 15 minutes.

Diffractometer Plots

In order to make visual comparisons easier, diffraction line intensities of the four powdered samples were plotted using diffractometer equipment. Plots were made in each case using Cu K-alpha radiation over the two-theta range of 18° to 45°. The plots appear in the appendix.

Line-Evaluation Procedure

Using different combinations of several of the most intense lines, entries were made into the Index to the Powder Pattern Diffraction File (27). The d spacings on all likely cards were compared with the experimentally obtained spacings in hopes of obtaining a

good fit with one card.

Metallographic Examination

Major experimental emphasis was placed on the metallographic examination of the interface. Changes in the microstructure as a function of temperature, time at temperature, and cooling program were examined by preparing normal and taper sections of the interface. An effective etchant and polishing procedure were also developed.

Effect of Temperature

Small chunks of glass were placed on pieces of ceramic measuring approximately $\frac{1}{4} \times \frac{1}{4}$ inch, and these were placed in a cold, resistance furnace. Suitable glass-ceramic bead seals were made by heating the samples to 800°, 900°, 1000°, 1100°, or 1200° C, holding the given temperature for eight hours, and then allowing the samples to cool with the furnace to room temperature. Cooling required about 12 hours.

Effect of Time at 1200° C

The effect of time at 1200° C on the F66-glass seal was studied by holding samples similar to those mentioned above at 1200° C for different lengths of time. These time intervals included 5 sec.,

4 hrs., 8 hrs., 12 hrs., 20 hrs., and 25 hrs. All samples were furnace-cooled to room temperature.

Effect of Cooling

Ten 1/8 × 1 inch disks of F66 were each placed in a small wire holder, topped with glass, heated to 1200° C, and held for ten hours. The furnace was turned off, and as it cooled past certain temperatures, samples were removed and allowed to continue cooling in air. Temperatures at which a sample was removed were 1200°, 1100°, 1000°, 900°, 800°, 700°, 600°, 400°, 200°, and 20° C.

Mounting and Procedure

All samples were mounted in transoptic plastic. Their orientation was such that a normal section through the interface could be observed. In the case of F66 samples displaying any of the new phase, taper sections were prepared in an attempt to bring out added detail. Better results were obtained by mounting the taper samples with the ceramic on top; the view, then, was looking past the ceramic into the glass at the interface. Although techniques are available for making accurate 10:1 tapers, none was applied because of the extra time required (23).

Polishing Procedure

Successive stages in polishing were 120 mesh wet-belt grinder, 300 and 400 mesh wet emery paper, 600 mesh lapping paper, six-micron diamond paste on a lap wheel surfaced with hard paper, and one-micron diamond paste on a similar wheel. Kerosene was used as a lubricant. About ten samples could be lapped before the paper became too soft. With the exception of two or three alumina samples, no difficulties were encountered in obtaining a flat, scratch-free surface.

Etching Procedure

A trial and error method was used in the search for an effective etchant. Common to all trials was HF. Most satisfactory results were obtained by using B-etch, a solution of ten parts HF, 45 parts HNO_3, and 45 parts water. Following the final polishing operation, the excess kerosene was wiped off, the etch was carefully swabbed on for about one second, and the surface was cascade-rinsed in distilled water and dried with hot air.

Examination Procedure

All polished samples were examined under various combinations of light intensity, magnification, and light filters (23).

Sensitized light, polarized light, and oblique light were also employed. Representative photographs were taken using polaroid pos-neg film packets. Average exposure times were two to three seconds, and the development time was 20 seconds.

Tensile Test

There are two problem areas associated with the testing of a brittle substance in tension. They are (1) how to apply a uniaxial tensile force, and (2) how to hold a brittle specimen so as to avoid stress concentrations. The high temperatures necessary for making the seals and the slightly irregular final shapes of the specimens further complicated the problem. To overcome the first problem area, a hydrostatic test was selected (4). A partially successful attempt was made to solve the second problem area by using a variety of stress distributors, pads, and protectors. After the specimens failed, the fracture surfaces were examined stereographically and metallographically in an effort to discover the section of the seal through which fracture was propagated.

Specimen Design

The test specimen consisted of a 3/4 inch outside diameter ceramic tube one inch long with 1/8 inch walls. A ceramic disk one inch in diameter and 1/8 inch thick was sealed to each end of the

cylinder using a glass washer of 3/4 inch outside diameter, 1/2 inch inside diameter, and 1/16 inch thickness. The ceramic disk at one end had a 1/8 inch hole in the center. The five pieces for each specimen were stacked in a cold furnace with the holed disk on the bottom and then fused for 15 minutes at a temperature ranging from 800° to 1200° C. All samples were allowed to cool with the furnace.

Fixture Design

The testing fixture was basically a 1/2 inch hydraulic cylinder and piston, a small air reservoir, and a pressure line leading to the sample. Figure 4 is a schematic of the whole system, and Figure 3 shows some of the details. The working fluid was SAE 30 motor oil. A smoother application of pressure was possible when all air was removed from the system, including the sample, prior to each test. Pressure was applied using a 60,000 pound Baldwin testing machine which had the advantage of an infinite selection of load rates. The rate was adjusted to keep the time to rupture approximately one minute (26).

In testing the alumina samples, pressures up to 14,000 psi were obtained with no signs of leakage. While testing the steatite samples, however, considerable difficulty was experienced in preventing leakage around the teflon washer. Tension on the four through-bolts was either insufficient to prevent leakage or sufficient

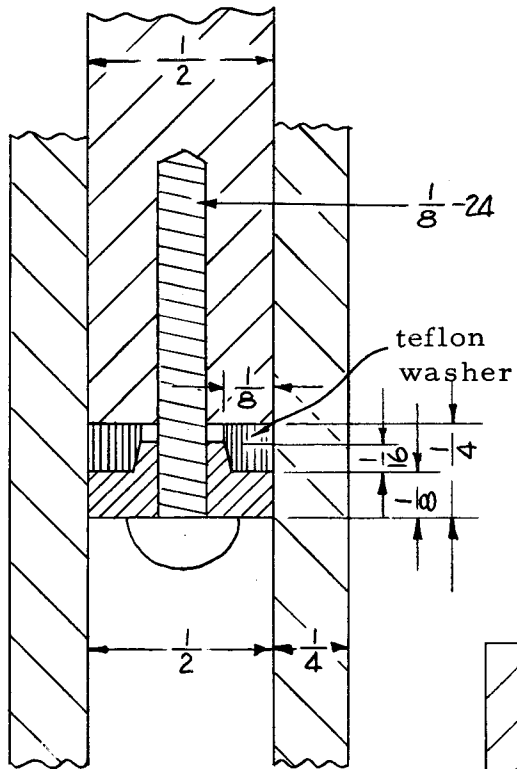

washer machined with
negative tolerance of
0.004 in.

Figure 3. Piston details.

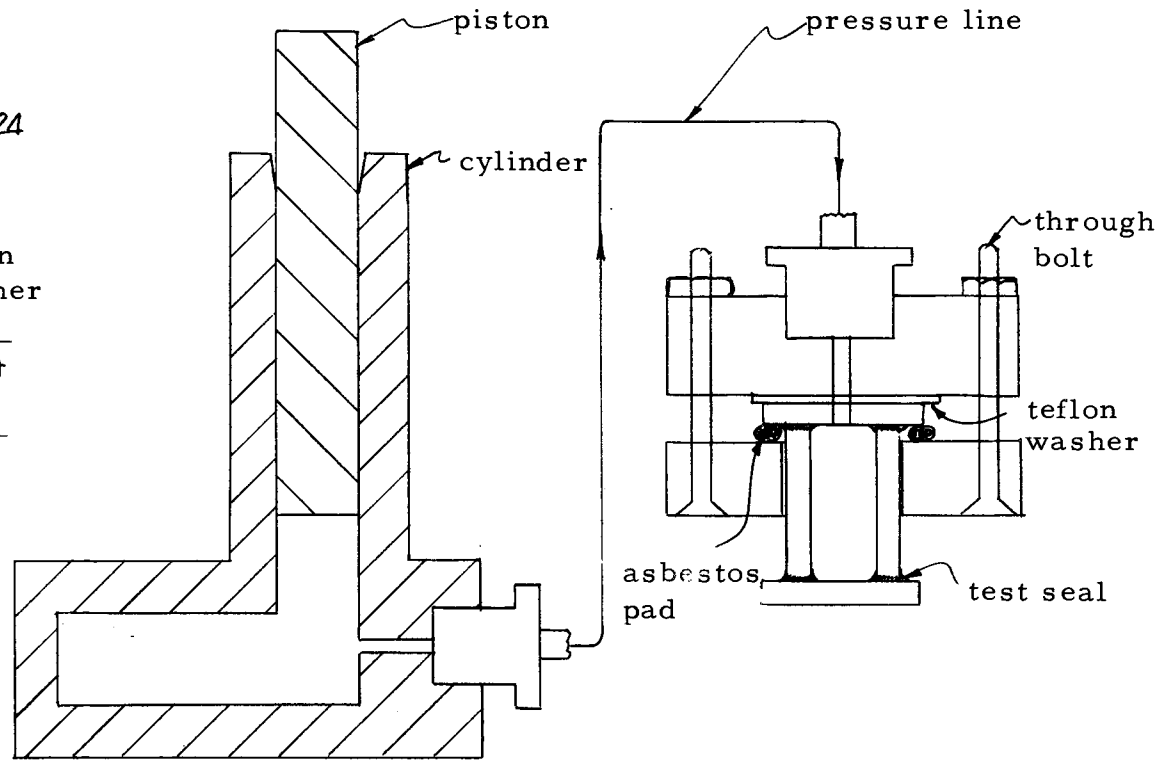

Figure 4. Schematic of hydrostatic pressure system.

to cause premature fracture to initiate within the relatively weak steatite. Many combinations of gasket and padding materials were used, but valid results were obtained on only two of the 15 total steatite samples. All samples were washed in an oil solvent prior to examination of the fracture surface.

Fracture Surface Observations

Each of the 30 fractured tensile specimens was carefully examined visually using a stereographic scope with a 3-power magnification. Using the characteristic topographical features of glass fracture surfaces mentioned earlier, an attempt was made to determine the point of origin and the direction of crack propagation. Four representative specimens were glued back together, sectioned on a diamond saw, mounted, and polished. These were examined under higher magnification in an attempt to see whether the crack propagated along the interface or through the glass or ceramic phase.

IV. EXPERIMENTAL RESULTS

The x-ray diffraction examination of the interfaces of both glass-ceramic systems strongly suggested the formation of a new compound at high temperatures. Metallographic examination of the F66-glass system confirmed this indication, but new phases were not positively identified at the interface of the Al_2O_3-glass system. The hydrostatic tensile tests of the seals in the F66 system were inconclusive because of difficulties with gripping the sample, but an analysis of variance of the rupture strengths of the Al_2O_3 seals showed a positive increase in strength with an increase in firing temperatures. The examination of the fracture surfaces indicated that fracture did not generally prefer the actual interface.

X-Ray Examination

The formation of a new compound in the interfacial region was strongly suggested by the obvious difference between the diffraction pattern of each ceramic and that of its corresponding glass-ceramic system. The four diffractometer plots are presented in the appendix.

Al_2O_3-Glass System

The d spacing found experimentally in the alumina ceramic made a near perfect match with those found on card 11-661 as seen

in Table VI. Most of the impurities in the ceramic are probably part of the binder and are in the glassy state. Impurity lines were therefore not detected; missing lines were apparently the result of low intensities.

By using the index and accompanying data cards (27), the experimental Al_2O_3-glass pattern was found to closely resemble either an aluminum borate (card 9-248) or an aluminum silicate (cards 6-0254 and 10-369). Table VII indicates a close, but not perfect, match with each card. In the Al_2O_3-glass pattern, the appearance of lines at 3.47, 2.54, and 2.37 and the high intensity of the line at 2.08 can be explained by the presence of unreacted ceramic.

Table VI. Comparison of diffraction pattern of Al_2O_3 ceramic and diffraction data card 11-661 (alpha Al_2O_3).

Al_2O_3 Ceramic*		Card 11-661		Al_2O_3 Ceramic*		Card 11-661	
d, Å	I	d, Å	I	d, Å	I	d, Å	I
3.47	M	3.49	75	1.372	M	1.375	50
2.54	M	2.55	100	1.240	W	1.240	18
2.38	W	2.38	45	1.190	VW	1.190	7
		2.166	2	1.150	VVW	1.149	5
2.08	S	2.088	100	1.125	VW	1.127	4
		1.966	2	1.100	VW	1.100	9
1.735	M	1.741	50	1.078	VW	1.079	9
1.595	VS	1.603	90	1.043	S	1.043	16
		1.548	2	1.018	VVW	1.018	2
1.510	VVW	1.512	11	0.998	S	0.998	13
1.410	W	1.406	38	0.982	VVW	0.983	2

*Data taken from Debye Powder Pattern.

Table VII. Compounds with d spacings similar to those found in the alumina-glass system.

Alumina-glass experimental #		Aluminum borate card 9-248		Mullite card 6-0258		Aluminum silicate card 10-369	
d	I	d	I	d	I	d	I
3.47*	25	-	-	-	-	-	-
-	-	3.40	60	3.41	71	3.41	90
3.36	31	3.35	100	3.38	100	3.36	100
-	-	3.10	40	-	-	3.19	10
-	-	-	-	-	-	2.93	10
2.83	17	2.82	80	2.88	25	2.88	70
2.68	21	2.67	100	2.69	51	2.67	80
-	-	2.64	60	-	-	-	-
2.54*	25	-	-	2.54	60	2.53	90
2.50	19-	2.50	100	-	-	-	-
2.42	14	2.42	60	2.42	17	2.42	60
2.37*	19	-	-	-	-	2.37	10
-	-	2.30	60	2.29	24	2.30	30
2.26	14	2.27	40	-	-	2.28	60
-	-	2.25	80	-	-	-	-
2.18	21	2.17	100	2.20	75	2.20	100
-	-	2.16	60	-	-	-	-
2.11	17	2.10	80	2.12	29	2.10	60
2.08*	32	2.09	40	2.10	7	2.09	30

* Pure alumina lines.

Data taken from the diffractometer plot in the appendix.

The diffraction photograph taken of the ceramic-glass mixture heated at 1000° C for 25 hours was indistinguishable from the pure Al_2O_3; this indicates that a reaction had not yet taken place.

F66-Glass System

The F66 steatite ceramic proved difficult to interpret by x-ray diffraction methods because of the number of different components present and the resulting complicated pattern. No data card was found that even approximately matched the d spacings found experimentally in F66.

The radical change in structure caused by heating the F66-glass mixture to 1200° C again suggested the formation of a new compound. Many diffraction data cards were searched in an attempt to identify this new substance, but no positive results were obtained. As seen in Table VIII, portions of the new substance resemble a magnesium meta silicate or a potassium aluminum silicate hydrate. The latter substance is unlikely because of the small amount of potassium present in the F66-glass system.

Metallographic Examination

The strong indications of a new interfacial phase by x-ray diffraction studies encouraged a metallographic examination that could both reveal the nature of the interface as a whole and confirm

Table VIII. Compounds with d spacings similar to those found in the steatite-glass system.

F66-Glass[@]		Card 11-187[*]		Card 13-415[#]	
d, Å	I	d, Å	I	d, Å	I
4.39	46	-	-	4.41	12
3.28	49	4.32	40	3.29	50
3.25	49	3.25	100	-	-
3.17	78	3.18	100	3.17-	60
2.98	53	2.97	60	2.98	95
2.87	52	-	-	2.88	100
-	-	-	-	2.80	8
2.72	38	2.73	80	2.70	8
2.55	37	2.54	40	2.54	35
				2.52	35
2.45	37	2.42	40	2.46	60
				2.44	20
2.37	29	-	-	2.38	16
-	-	-	-	2.34	8
2.30	31	-	-	2.29	2
-	-	-	-	2.21	20
				2.20	20
2.11	31	-	-	2.11	45

[*] Potassium aluminum silicate hydrate.

[#] Magnesium meta silicate.

[@] Data taken from diffractometer plot in appendix.

the existence and identify the origin of any new phase. An imperative first step was the development of an etchant that could effectively bring out the new phase. Studies of the effect of temperature, the effect of time at temperature, and the effect of cooling followed. Limited evidence of a new phase in the Al_2O_3 system was found. An obvious new phase was found in the F66 system. Its origin is probably related to diffusion effects.

Etchant

A trial and error search for an effective etchant producted B-etch, a mixture which is normally used in work with refractory materials. The effect of this etchant can be seen in Figures 5 through 8.

Effect of Temperature

In the Al_2O_3-glass seals, the width of the glass-affected ceramic zone increased with temperature, but the glass phase underwent no change. Both the ceramic and glass phases in the F66 system reflected several extensive changes with temperature. For both systems, the observations and their probable explanations are presented.

Observations in the Al_2O_3-Glass System. The temperature at which the Al_2O_3-glass seal was formed had little effect on the

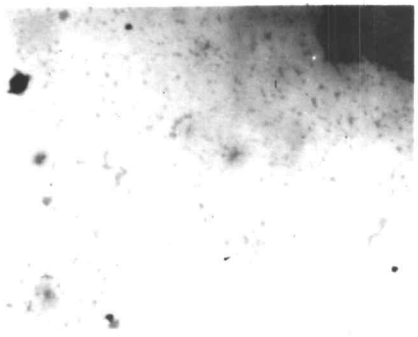

Figure 5. Al_2O_3 seal heated at 1200°C for 8 hrs. and furnace-cooled. No etch, 500X.

The small black voids stand out clearly, but the Al_2O_3 crystals and the glassy binder lack definition.

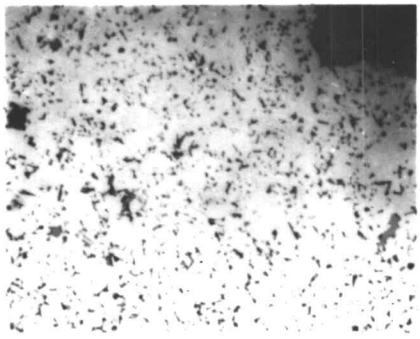

Figure 6. Al_2O_3 seal heated at 1200°C for 8 hrs. and furnace-cooled. B-etch, 500X.

Good definition between the crystalline and glassy phases of the ceramic is achieved.

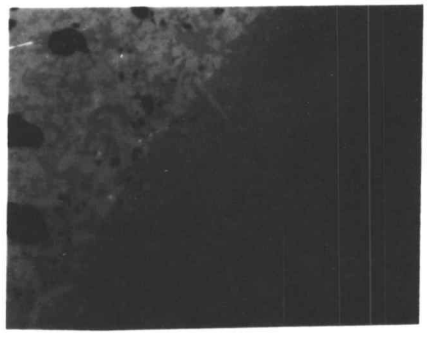

Figure 7. F66 heated at 1200°C for 4 hrs. and furnace-cooled. No etch, 250X.

The interfacial region shows no evidence of the dark band or the glass-affected ceramic zone. The new phase is just faintly visible.

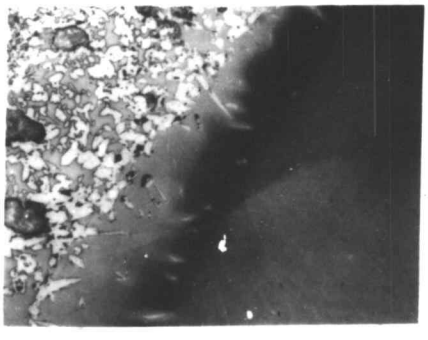

Figure 8. F66 seal heated at 1200°C for 4 hrs. and furnace-cooled. B-etch, 250X.

The new phase, dark band, and glass-affected ceramic zone are all clearly defined.

observed microstructure. As seen in Figures 9, 10, and 11, there are some small crystals growing from the ceramic into the glass in the seals made at 800°, 900°, and 1000° C. Also, glass is apparently interpenetrating the ceramic body and filling some of the voids near the interface. This latter effect increases noticeably with temperature.

Explanation of Observations. The habit of the small crystals growing at the interface suggests a material with a crystal system classified as orthorhombic, tetragonal, or cubic. All three substances identified in Table VII have orthorhombic crystal systems.

The absence of large-scale devitrification is to be expected. The glass network should be able to incorporate a large amount of an intermediate oxide. The new alumino-silicate glasses have compositions with over 20 percent Al_2O_3 (18).

None of the alumina button-seals cracked upon cooling. The relative coefficients of thermal expansion for 7052 glass and alumina ceramic cause the ceramic to take up tensile stresses. However, even near the interface, the glassy part of the ceramic phase, although in tension, is only a small portion of the ceramic, and it is not continuous. Cracks cannot propagate within this discontinuous phase.

Observations in the F66 System. The effect of temperature on the interfacial microstructure can be seen in Figures 14 through 18.

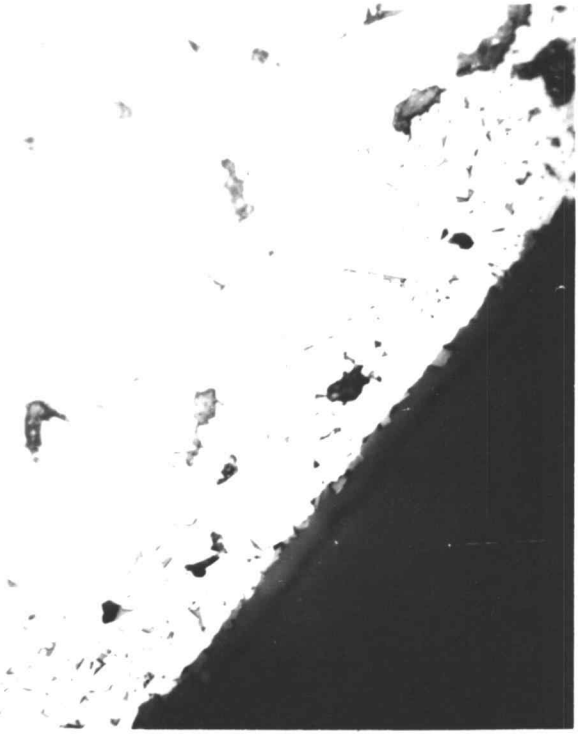

Figure 9. Al_2O_3 seal heated at 800°C for 8 hrs. and furnace-cooled. 500X.

Large voids in the ceramic phase are randomly distributed with the possible exception of a narrow zone of about ten microns at the interface. Small crystals of irregular orientation and shape are growing from the ceramic into the glass. A weak band is on the glass parallel to the interface.

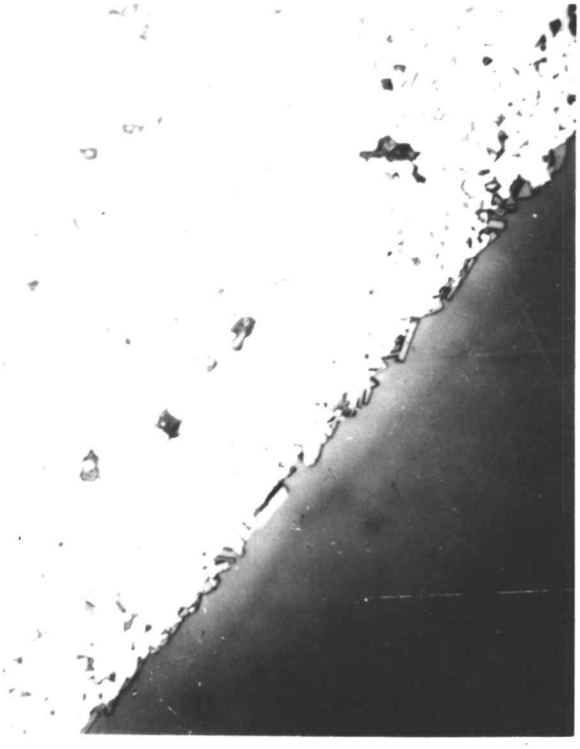

Figure 10. Al_2O_3 seal heated at 900°C for 8 hrs. and furnace-cooled. 500X.

The void-free zone is now about 30-40 microns wide. The small crystals growing into the glass have developed angles near 90° and their density of distribution is greater. The interface is generally more irregular than before.

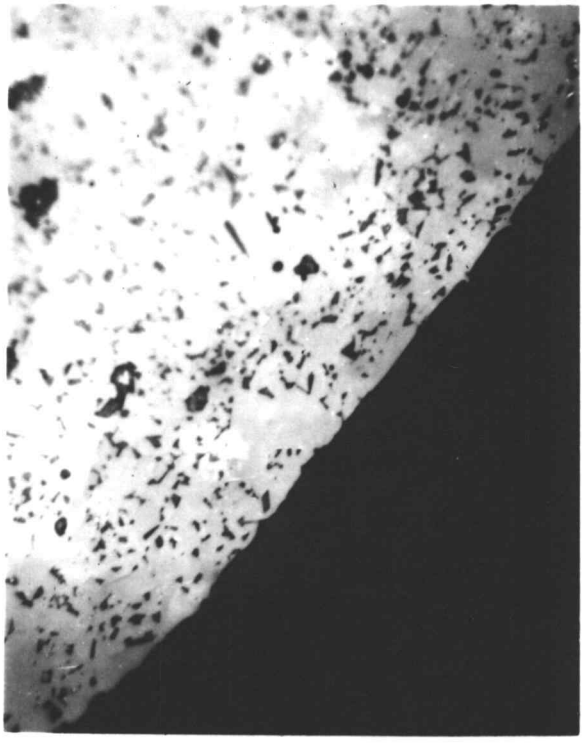

Figure 11. Al_2O_3 seal heated at 1000°C for 8 hrs. and furnace-cooled. 500X.

The void-free zone is now approximately 60 microns wide. The crystals, although less dense, again appear with angles near 90°. They frequently appear to develop on projections of the ceramic into the glass. The three specks in the glass phase are probably inclusions.

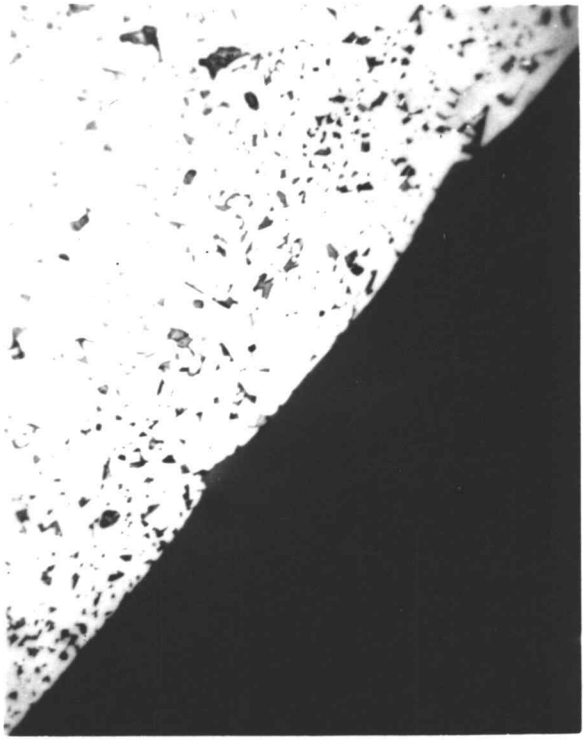

Figure 12. Al_2O_3 seal heated at 1100°C for 8 hrs. and furnace-cooled. 500X.

The zone is now approximately 80 microns wide. The crystals are no longer visible.

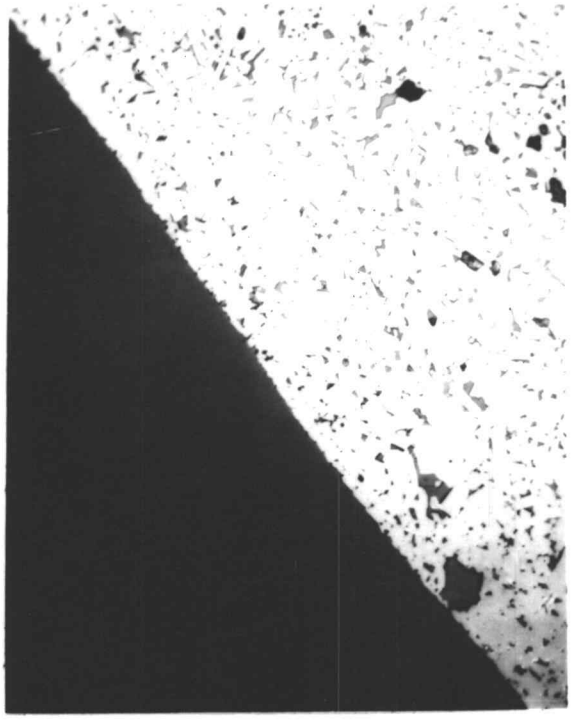

Figure 13. Al_2O_3 seal heated at 1200°C for 8 hrs. and furnace-cooled. 500X.

Excepting that almost the whole ceramic area is within a zone where glass has penetrated, there is little change from Figure 12. No crystals are visible at the interface.

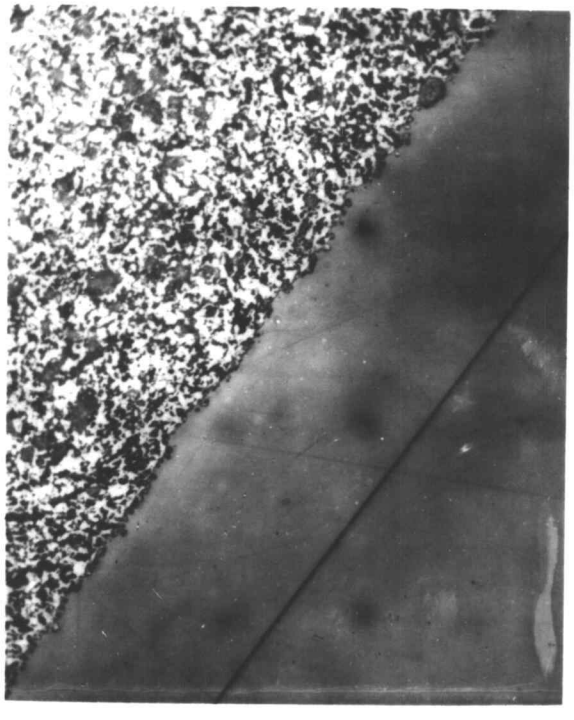

Figure 14. F66 seal heated at 800°C for 8 hrs. and furnace-cooled. 250X.

The interface shows little or no diffusion effects. No crystals have formed in the glass phase. A long crack can be seen in the glass phase.

Figure 15. F66 seal heated at 900°C for 8 hrs. and furnace-cooled. 250X.

The interface is now slightly more irregular, and there is evidence that glass has flowed into the ceramic voids along the interface.

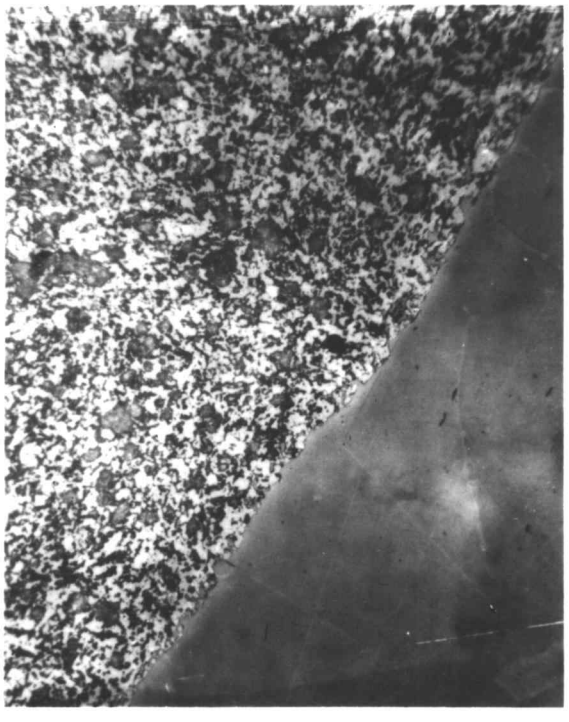

Figure 16. F66 seal heated at 1000°C for 8 hrs. and furnace-cooled. 250X.

There is a zone about 20 microns wide where an apparent flow of glass into the ceramic has occurred. Some small ceramic particles seem nearly detached from the main phase.

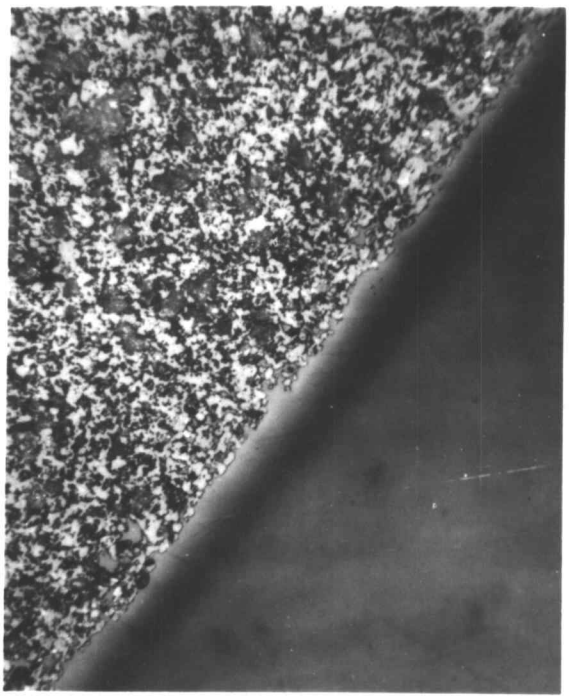

Figure 17. F66 seal heated at 1100°C for 8 hrs. and furnace-cooled. 250X.

The interface is still more irregular and the glass-affected zone within the ceramic phase is now nearly 30 microns wide. In the glass phase, a dark band is present parallel and close to the interface. Crystals have not yet formed within the glass phase.

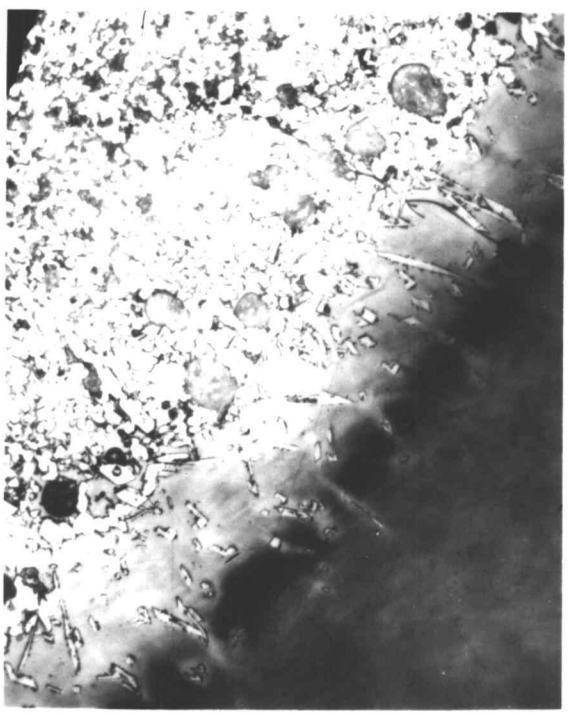

Figure 18. F66 seal heated at 1200°C for 8 hrs. and furnace-cooled. 250X.

The zone within the ceramic phase is now about 100 microns wide. Large round voids have developed within this region. Within the glass phase the band has darkened and moved away from the interface, and many small angular crystals have formed.

Several changes are noted as temperature is increased: (1) The width of the glass-affected ceramic zone increases. (2) In the glass phase, a shaded band develops parallel to the interface; at 1100° C it is only faint, but at 1200° C, it is dark. (3) Large voids, which appear black in the photographs, increase in frequency. (4) In seals made at 1200° C, macrocracks appear as the specimen is cooled to room temperature. (5) Although it cannot be seen in the black and white photographs, a faint blue coloration develops within the glass. (6) At 1200° C, a new phase develops within an area of the glass that is bounded by the dark band and the ceramic.

Explanation of Observations. Explanations for most of the observations enumerated above are based on probable diffusion effects.

The decreased viscosity has enabled the glass to penetrate the porous ceramic body and fill some of the voids. The width of this zone is measured in each of the Figures 14 through 18.

The dark band could be the result of a higher rate of attack on a region where a diffusion-caused change in composition produced a glass of less resistance to acid attack. This characteristic is typical of glasses which contain an overabundance of Na and Ca ions (16).

The increased number and size of black voids in Figures 14 through 18 are probably the result of outgassing of the porous ceramic. High-temperature soaking is a common technique for driving out entrapped gasses in ceramic vacuum tubes (4).

Figure 19 demonstrates crack size, length, location, orientation and density. Glass is much weaker in tension than in compression.

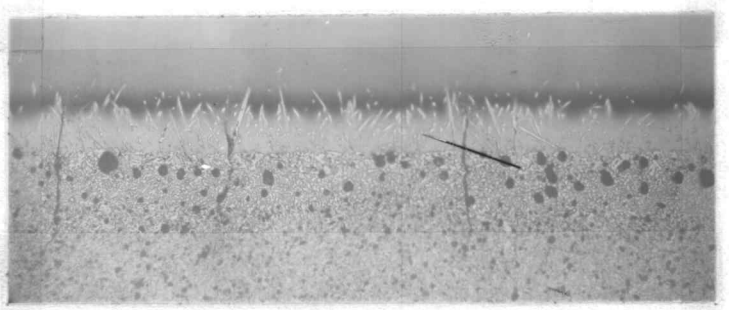

Figure 19. Cooling cracks in F66 seal heated to 1200° C and furnace cooled. 37X.

> The fact that the cracks are perpendicular to the interface indicates that the tension field is in a horizontal plane. The cracks extend up into the glass, but do not penetrate the dark band; they extend down into the ceramic, but do not penetrate much beyond the glass-affected zone. Higher magnification shows them to be intergranular.

Nearly all glass failures are initiated at an imperfection which lies in a tension field. Because of the relative coefficients of expansion of 7052 glass and F66, cooling the seal below the setting point of glass, 456° C, causes the glass to be placed in compression and the ceramic in tension (5). It is felt that crack initiation occurs within the glass-affected ceramic zone which is probably in tension. Inspection of this zone in samples that have been held at 1200° C for some time reveals a continuous glass matrix where a crack might

easily start. Closer inspection shows that these cracks do not traverse the stronger ceramic crystals but prefer to propagate within the glass matrix or along the ceramic crystal boundaries. The cracks do not extend into the unaffected ceramic probably because of its superior strength properties. They do extend past the seal interface into the glass, but they do not protrude beyond the dark band. The energy that represents the stresses that a crack relieves may help to extend the crack slightly into glass which is in compression, but it is apparently not adequate to extend it into the sound, unaffected body of the ceramic.

The light blue coloration seen in samples heated to 1200° C may be caused by metallic impurity atoms that have diffused into the glass from the ceramic. Copper causes a blue color in glass when it is present in amounts of as little as 0.006 percent. The effect is intensified by the presence of barium, boron, or lead (1).

The new phase found in seals heated to 1200° C is either the result of chemical reaction or devitrification, but in either case, it is probably initially made possible by diffusion. Local changes in composition are normally the cause of accidental devitrification (18). Apparently, the components of the F66 attain a high degree of mobility at this temperature and are able to diffuse into and be dissolved by the glass phase. Since the composition changes are essentially the modifier oxides, MgO and BaO, their permanent incorporation

into the glass network is not likely. There is a good chance that they would precipitate out during slow cooling. In an electron microprobe traverse across a similar seal, Welty found a peak in Mg content in the glass phase near the interface (29).

Examination of New Phase in F66 System

Two further examinations, the effect of time and the effect of cooling, were undertaken to help ascertain whether the new phase seen in the F66 system was a chemical reaction product or a duffusion-caused devitrification product. Examination of the effects of cooling gave strong evidence favoring the latter.

Effect of Time at 1200° C. Although a normal section and 10:1 taper section were photographed at each of the six time intervals, no positive conclusion as to the origin of the new phase was reached. Figures 20 through 22 show that the new phase is present after only five seconds at 1200° C and that the amount is relatively unchanged after four hours. Either a chemical reaction has gone to completion or a supersaturated component has precipitated out to equilibrium. The dark band becomes more diffuse with longer time at temperature. This effect could be caused by a decrease in the slopes of the composition gradients across the interface. Also, the relatively fluid glass has been more easily able to interpenetrate the crystalline portion of the ceramic. The width of this

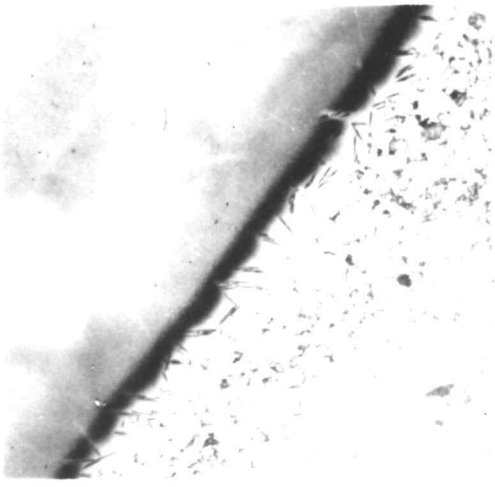

Figure 20. F66 seal held at 1200°C for 5 sec. and furnace-cooled. 250X.

The ceramic zone into which the glass has penetrated is approximately 10 microns wide. The crystals in the glass phase are quite dense but have essentially only one dimension. The band is very dark and narrow and is close to the interface. The zone in which crystals are growing is about 30 microns wide.

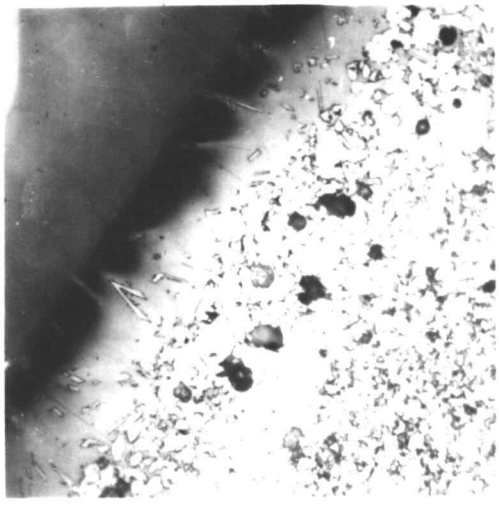

Figure 21. F66 seal held at 1200°C for 4 hrs. and furnace-cooled. 250X.

The glass-affected ceramic zone is now about 100 microns wide and large round voids are present. The interface is extremely irregular. The crystals have grown considerably and developed their characteristic habit. The band is less dense and further removed from the interface. The crystal zone is now approximately 60 microns wide.

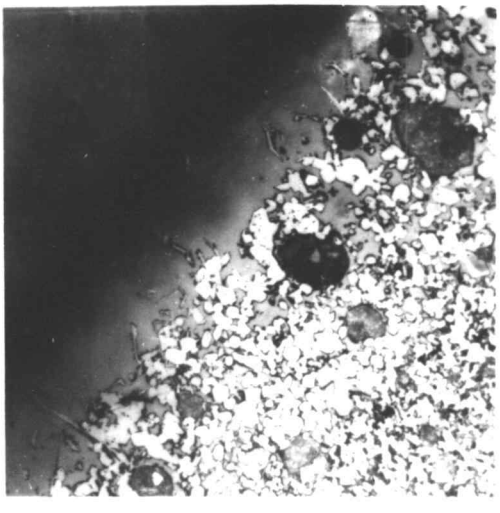

Figure 22. F66 seal held at 1200°C for 12 hrs. and furnace-cooled. 250X.

The glass-affected ceramic zone is about 130 microns wide, and the round voids are enlarged. The band is more diffuse, and the crystal zone is 70 microns wide.

glass-affected ceramic zone increases with each increase in time.

The Effect of Cooling. Of the ten pictures taken of the F66 samples quenched from different temperatures, only the first four show significant changes. They are presented as Figures 23 through 26. Samples quenched from temperatures below 900° C yield pictures very similar to Figure 26. These figures suggest that the origin of the new phase is in a divitrification mechanism. Apparently extensive diffusion of ceramic components into the glass occurs at 1200° C. The resulting changes cause some of the components of the ceramic-affected glass to fall outside of their limit of "solid" solubility, and if they are cooled slowly enough they precipitate out as devitrification products. The fact that Figure 23, a sample quenched from 1200°, shows no crystals suggests that this temperature is too high for the stability of a nucleus.

Tensile Test

A combination of the information gained from the tensile test and the fracture surface examination confirms that strong seals were obtained in both ceramic systems at temperatures of 900° C and higher. The method of supporting the test specimen in the fixture was satisfactory only for the alumina seals. Examination of the fracture surfaces showed that crack propagation generally preferred the glass phase rather than the seal interface.

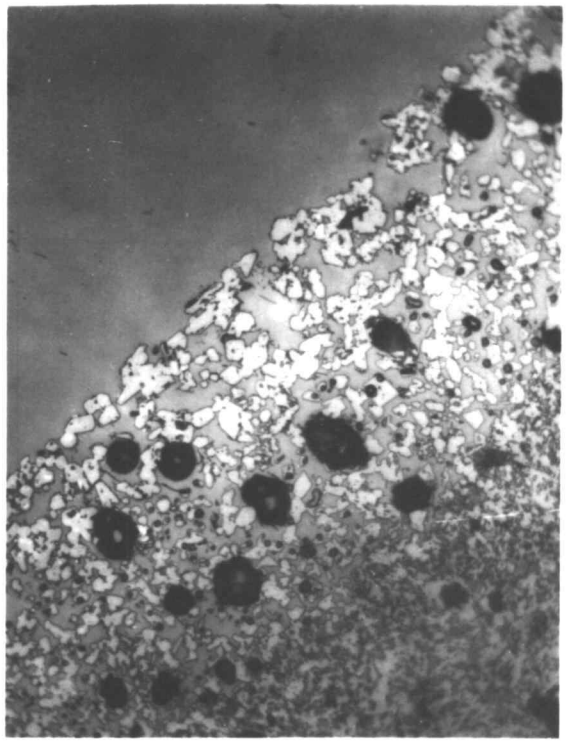

Figure 23. F66 seal heated at 1200°C for 12 hrs. and air-cooled. 250X.

Although the ceramic microstructure indicates that considerable diffusion into the glass has occurred, the air-quench from 1200°C has prevented devitrification. The dark band is also missing.

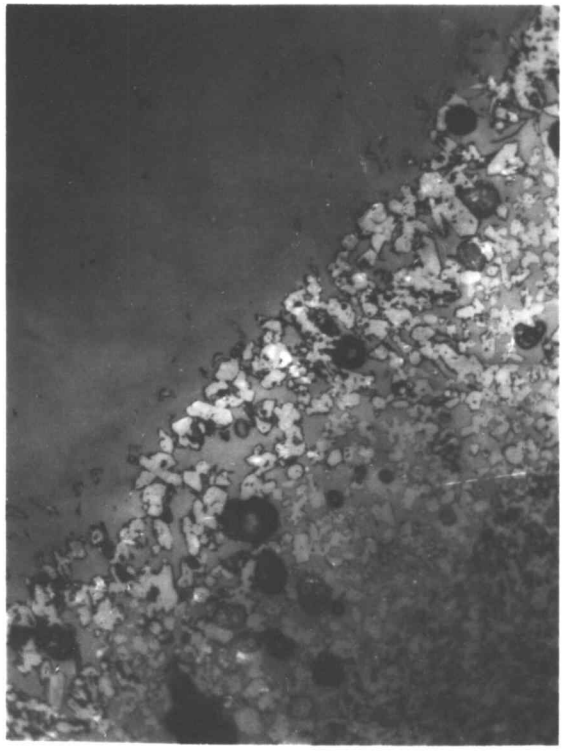

Figure 24. F66 seal heated at 1200°C for 12 hrs. furnace-cooled to 1100°C, and then air-cooled. 250X.

Very small crystallites can be seen along the interface. The slow cooling to 1100°C has provided a more desirable condition for nucleation and a longer time for some grain growth.

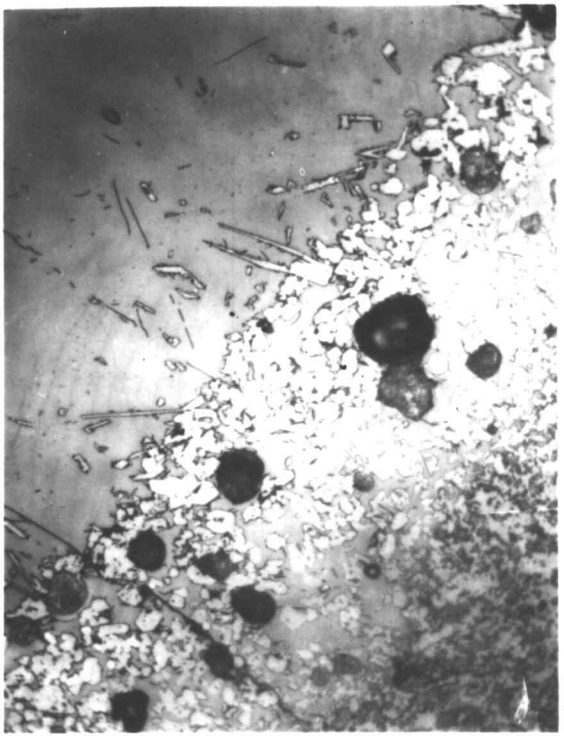

Figure 25. F66 seal heated at 1200°C for 12 hrs., furnace-cooled to 1000°C, and then air-cooled. 250X.

Although many of the crystals are yet too small, some are large enough to be recognizable by their characteristic habit.

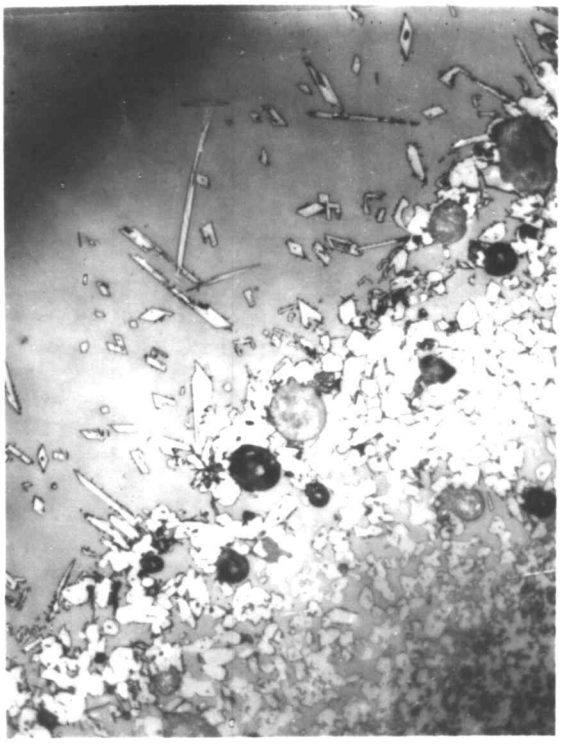

Figure 26. F66 seal heated at 1200°C for 12 hrs., furnace-cooled to 900°C, and then air-cooled. 250X.

The crystals have attained maximum size. The ones with a diamond-shape and a centered black speck appear very similar to barium disilicate (13). No x-ray evidence of this compound has been found. Furnace-cooling to temperatures below 900°C produced a microstructure similar to this figure.

F66

In all but two of the 15 samples, failure occurred for reasons other than internal hydrostatic pressure. In most of the cases, failure was at the wrong end of the sample; this suggested that damage occurred while the sample was being bolted to the fixture. In other cases, the ceramic tube crushed in the middle, and no portion of the seal was broken. A recommended design improvement for the specimen is presented in Chapter VI.

Al_2O_3

In all but two cases, the strength data collected in testing each alumina sample were considered valid. Not all the increase in strength for each rise in temperature was due to an improvement in the bond. Some was due to both the improved fillet shape and the increased seal area as the glass became more fluid.

Table IX. Rupture strength, in pounds, for alumina-glass seals formed at various temperatures.

Temperature of seal formation	800°	900°	1000°	1100°	1200°
Observations	0	429	981	x	2125
	0	x	1000	970	2720
	0	600	1170	2025	2615

x Specimen ruptured incorrectly.

An analysis of variance shows that for the data in Table IX, despite the wide variance within each treatment, an improvement in rupture strength with temperature can still be easily detected. The calculation of the F-statistic appears in the appendix, and it shows that F_{obs} is 41.6 and $F_{5\%}$ is 3.8 (17). Even if it is assumed that wetting of the ceramic by the glass increases the seal area by 100%, further calculations (appendix) show that the interface withstands stresses up to 5200 pounds per square inch. This indicates that the seal is as strong as the glass. While examining these data and calculations, it must be remembered that the results are, at best, only qualitative (26). They are extremely sensitive to surface conditions, specimen shape, and loading rate. Quantitative results should not be attempted with less than 20-30 samples for each treatment (26).

Fracture Surface Examination

The sketches of typical fracture surfaces in Figure 27 and the photographs in Figures 28 through 30 show that cracks generally propagate through the glass phase. In most of the specimens, the point of origin of the crack was not found. For some even the direction of crack propagation was difficult to determine. In the cases where the proper seal failed, the propagation direction appeared to be inside to outside, as would be expected. Typical fracture shapes for high temperature alumina specimens were as shown

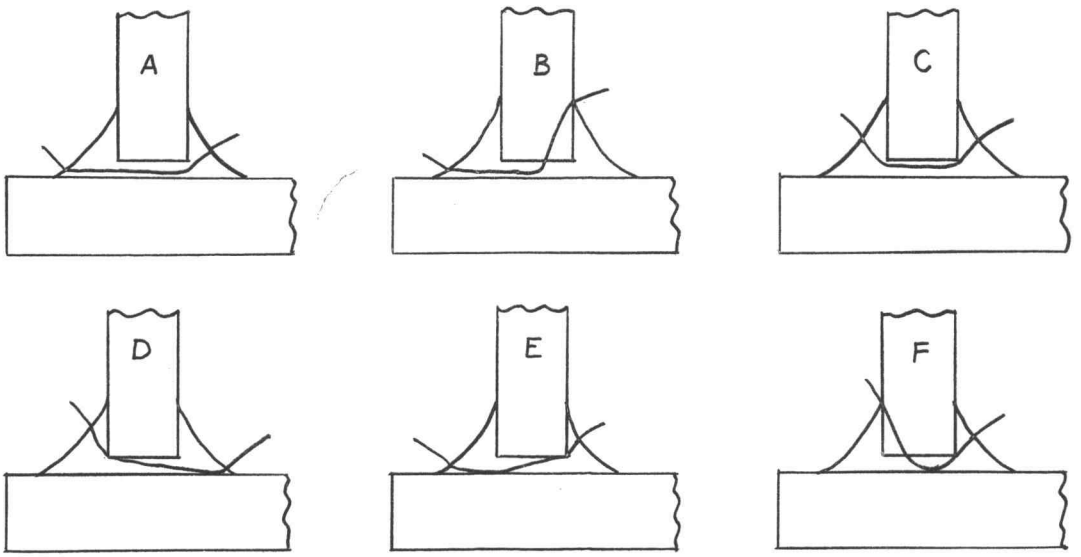

Figure 27. Typical cross-sections through fractured seals.

in Figures 27 A, B, and E. The seals made at 900° C favored shape C. The steatite seals either failed in the ceramic phase or as depicted by shapes D and F.

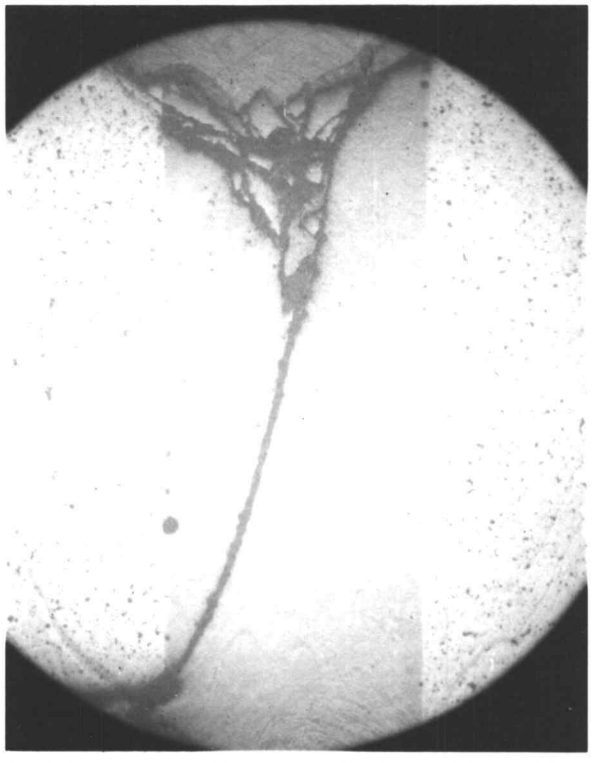

Figure 28. Cross-section of Al_2O_3 seal formed at 900°C. 25X.

The wider glass phase is clearly shown for this seal made at a low temperature. Crack propagation occurred from inside to outside and remained within the glass phase. An overall view of this specimen appeared similar to Figure 27C.

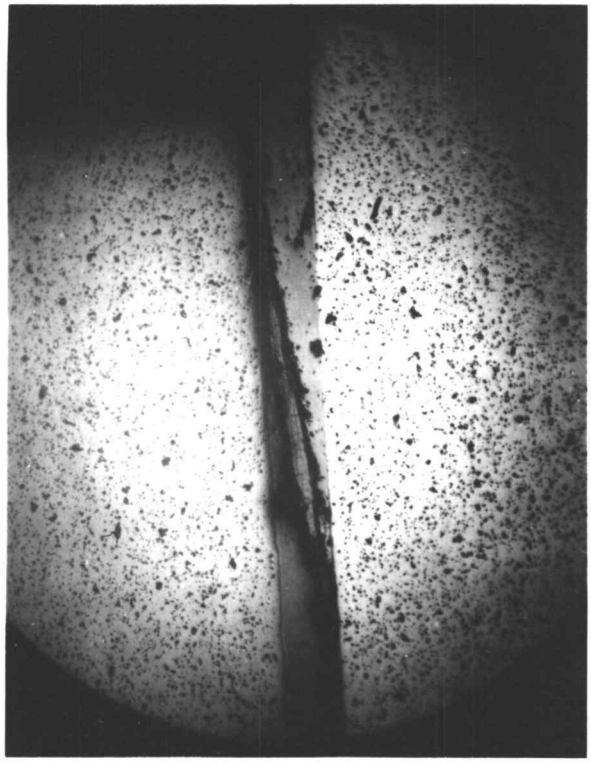

Figure 29. Cross-section through Al_2O_3 seal formed at 1200°C. 25X.

A very thin layer of glass can be seen between the two ceramic parts. This sample broke into about 50 pieces. Neither the crack origin nor the propagation direction could be determined. Failure occurred for only a short distance along the actual interface.

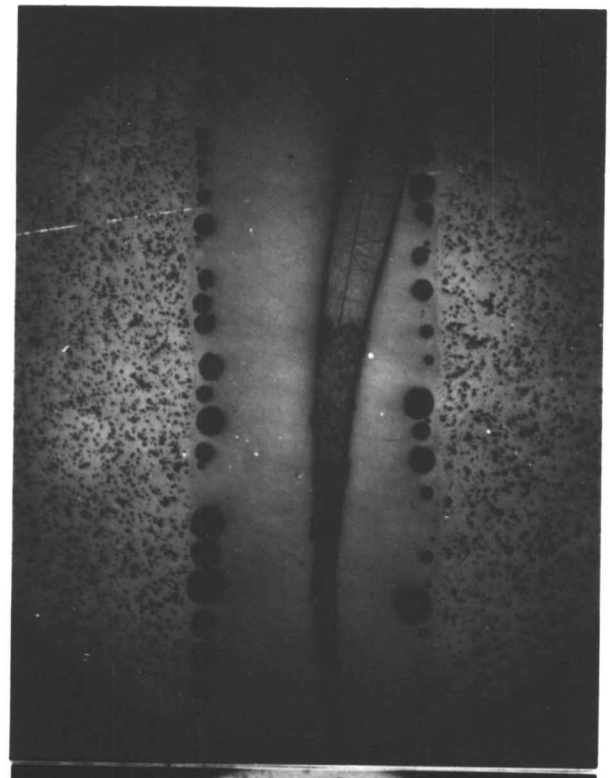

Figure 30. Cross-section through F66 seal formed at 1000°C. 25X.

This sample failed at the end being gripped. Although the direction of crack propagation could not be determined, the phase through which it passed is obviously glass.

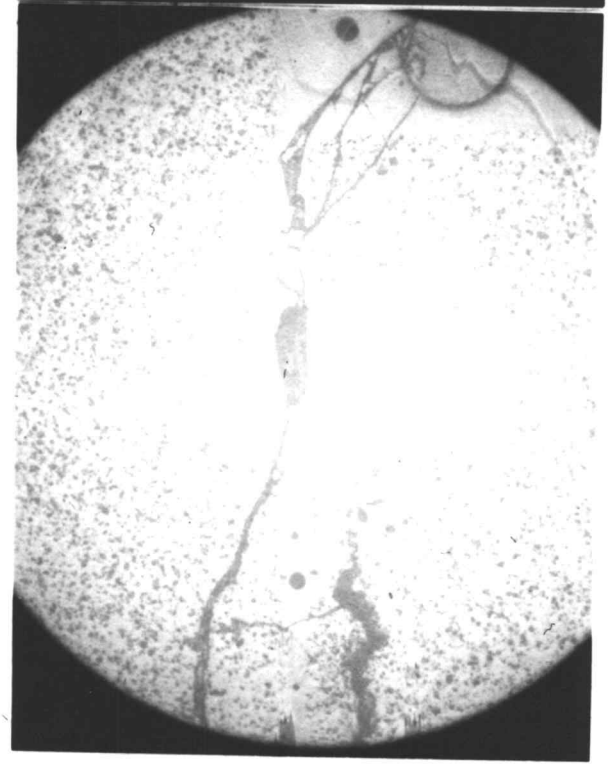

Figure 31. Cross-section through F66 seal formed at 1200°C. 25X.

In this sample, the crack initiated in the glass on the outside at the end gripped by the fixture. The crack produced a final cross-section similar to Figure 27D. Propagation was through both the glass and ceramic phases.

V. CONCLUSIONS

Each examination performed in this project indicated that good adherence exists between 7052 glass and the ceramic F66 steatite or Al_2O_3 alumina. It is felt that the actual mechanism which produces this adherence must be similar to the one outlined by Pask for glass-metal systems.

Indications of Adherence

Each of the examinations gave evidence supporting good adherence. The x-ray diffraction powder patterns showed obvious differences between the original material and the interface material. This information suggested that some chemical bonds may be formed at the interface at high temperatures. Authors generally agree that good adherence in a glass or ceramic system can only be achieved with a chemical bond across the interface.

The metallographic examination of the F66-glass interface revealed a graded zone of transition from the steatite to the 7052 glass. At 1200° C some divitrification products were noted. Although the transition zone was not nearly so wide in the Al_2O_3-glass system, no sharp discontinuity appeared. Only limited evidence of a new interfacial phase was found. Thus, a continuous and coherent transition zone, deemed by Pask so important for adherence, was thought

to exist for both of the glass-ceramic systems studied. The rupture strength tests for the Al_2O_3 system provided convincing evidence that higher temperatures produced stronger seals. For the F66 system, few data points were obtained because of the difficulty in gripping the brittle ceramic. Examination of the fracture surfaces of the ruptured specimens showed that the crack origin was often at the interior of the specimen and the propagation was generally through the glass phase rather than along the interface. As mentioned in Chapter II, Pask feels this indicates that the solid-liquid surface energy is less than the solid-gas surface energy, and the energy of adherence is therefore large.

Proposed Mechanism

It is felt that oxygen plays a major role in providing good adherence in the ceramic-glass systems just as it does in providing good adherence in the glass-metal and ceramic-metal systems. There is a driving force for its incorporation into the molten glass, for it provides the silicon atoms with the increased screening they seek. At the same time, it is covalently bound in the ceramic phase as one of the oxide components. Thus, a chemical bond is established across the glass-ceramic interface.

VI. RECOMMENDATIONS

Certain experimental improvements and different approaches are recommended for an extended examination of adherence in the glass-ceramic system.

Experimental Improvements

In Figure 32, an improved design for the tensile test specimen is shown mounted in a schematic holder. Gripping of the portion of the cylinder on which the test seal is mounted is thereby avoided.

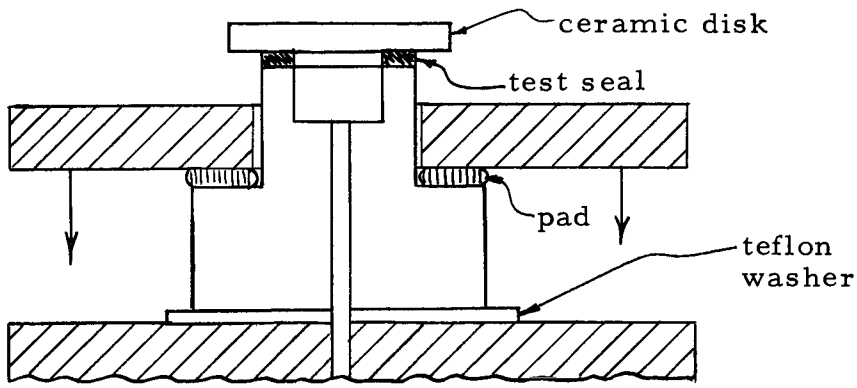

Figure 32. Improved design for tensile test specimen.

It is thought that a simple fused-silica jig could be designed that would prevent the ceramic disk from squeezing out all of the glass at the interface when fired at high temperatures. A glass seal of constant thickness would probably remove some of the variance

from the rupture-strength data.

The additional information derived from viewing taper sections was considered insignificant. It is felt that the application of this technique in the glass-ceramic system is unnecessary.

Project Extension

Further work should probably first be directed toward the examination of contact angles in various atmospheres and the identification of x-ray diffraction patterns using a diffractometer. Other work might include an examination of the migration of some of the components present. Essential to this work would be an electron microprobe.

BIBLIOGRAPHY

1. Angus-Butterworth, L. M. The manufacture of glass. New York, Pitman, 1948. 260 p.

2. Azaroff, Leonid V. Introduction to solids. New York, McGraw-Hill, 1960. 433 p.

3. Burke, J. E. and A. U. Seybolt. Procedures in experimental metallurgy. New York, Wiley, 1953. 329 p.

4. Clark, J. E. The use of ceramics in the construction of electron tubes and semiconductor devices. Allentown, Pa., Bell Telephone Laboratories, [1959]. 9 p. (Processed)

5. _____. The use of glass in the construction of electron tubes and semiconductor devices. Allentown, Pa., Bell Telephone Laboratories, 1959. 13 p. (Processed)

6. Cole, S. S. and G. Sommer. Glass-migration mechanism of ceramic-to-metal seal adherence. Journal of the American Chemical Society 44:265-271. 1961.

7. Condon, E. U. Physics of the glassy state. Part I. Constitution and structure. American Journal of Physics 22:43-53. 1954.

8. _____. Part II. The transformation range. American Journal of Physics 22:132-142. 1954.

9. _____. Part III. The strength of glass. American Journal of Physics 22:224-232. 1954.

10. _____. Part IV. Radiation-sensitive glasses. American Journal of Physics 22:310-317. 1954.

11. Dickson, J. H. (ed.) Glass. New York, Chemical Publ. Co., 1951. 300 p.

12. Eggers, D. F. et al. Physical chemistry. New York, Wiley, 1964. 764 p.

13. Holland, A. J. and Eric Preston. The microscopical examination and identification of crystalline products in commercial

glass. Journal of the Society of Glass Technology 21:395-408. 1937.

14. Kingery, W. D. Introduction to ceramics. 2d ed. New York, Wiley, 1963. 758 p.

15. _____. Metal-ceramic interactions. Part I. Factors affecting fabrication and properties of cermet bodies. Journal of the American Ceramic Society 36:362-365. 1953.

16. Kroeck, W. H. A short summary of glass technology and of the art of glass making and glass manufacturing methods. Allentown, Pa., Bell Telephone Laboratories, [1959]. 27 p. (Processed)

17. Li, Jerome C. R. Statistical inference. Vol. 1. 2d ed. Ann Arbor, Edwards, 1964. 565 p.

18. McMillian, P. W. Glass-ceramics. New York, Academic Press, 1964. 229 p.

19. Morey, George W. The composition of glass. Washington, Carnegie Institution of Washington, 1936. 18 p. (Supplementary Publication no. 23)

20. Pask, Joseph A. and Richard M. Fulrath. Fundamentals of glass-to-metal bonding. Part VIII. Nature of wetting and adherence. Journal of the American Ceramic Society 45:592-596. 1962.

21. Phillips, C. J. Get acquainted with glass. New York, Pitman, 1950. 235 p.

22. Pincus, A. G. Mechanisms of ceramic-to-metal adherence. Ceramic Age 63(3):16-32. 1954.

23. _____. Metallographic examinations of ceramic-metal seals. Journal of the American Ceramic Society 36: 152-158. 1953.

24. Pulfrich, H. Ceramic-to-metal seals. Ceramic Abstracts 18: 226. 1939.

25. Salmang, Hermann. Ceramics--physical and chemical fundamentals. 4th ed. London, Butterworth, 1961. 362 p.

26. Shand, E. B. Glass engineering handbook. 2d ed. New York, McGraw-Hill, 1958. 484 p.

27. Smith, Joseph V. (ed.) Index (inorganic) to the powder pattern diffraction file. Philadelphia, American Society for Testing Materials, 1964. 786 p. (Special technical publication 48-N2)

28. Warren, B. E. The basic principles involved in the glassy state. Journal of Applied Physics 13:602-610. 1942.

29. Welty, J. R. The nature of glass-to-ceramic adherence. Bell Telephone Laboratories Technical Memorandum MM-64-2832. 1964.

30. Zacharisen, William H. The atomic arrangement in glass. Journal of the American Chemical Society 54:3841-3847. 1932.

APPENDIX

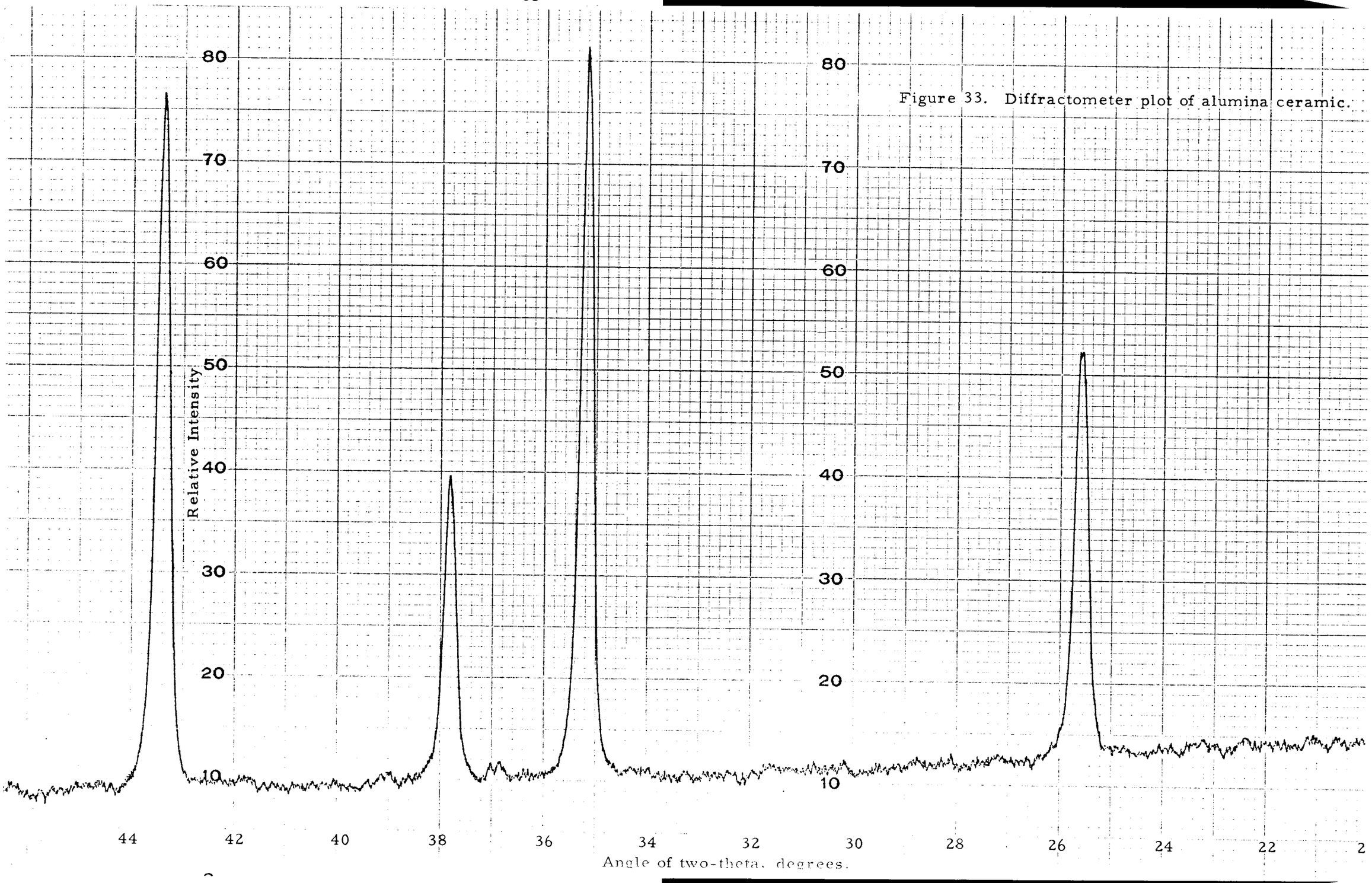

Figure 33. Diffractometer plot of alumina ceramic.

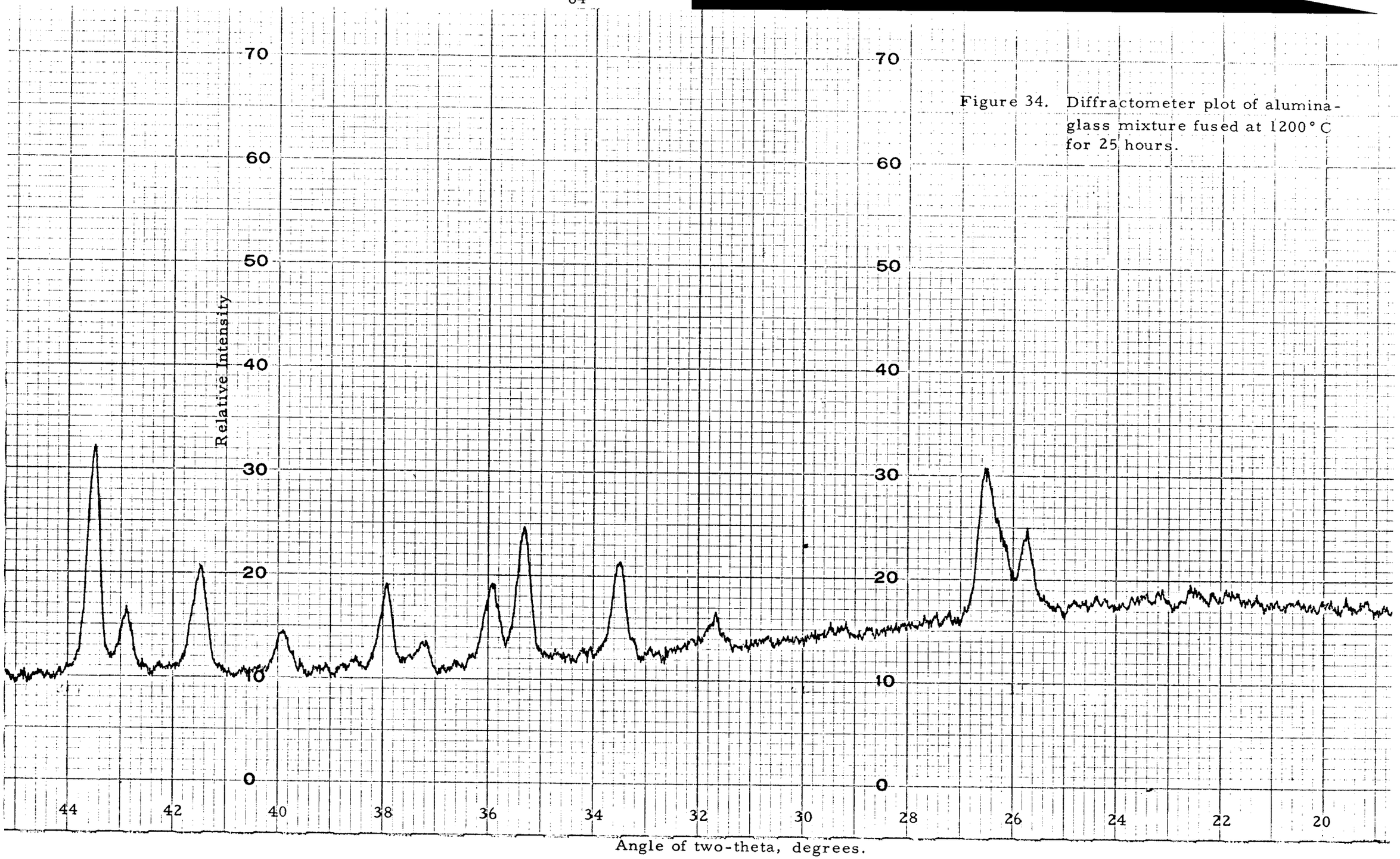

Figure 34. Diffractometer plot of alumina-glass mixture fused at 1200° C for 25 hours.

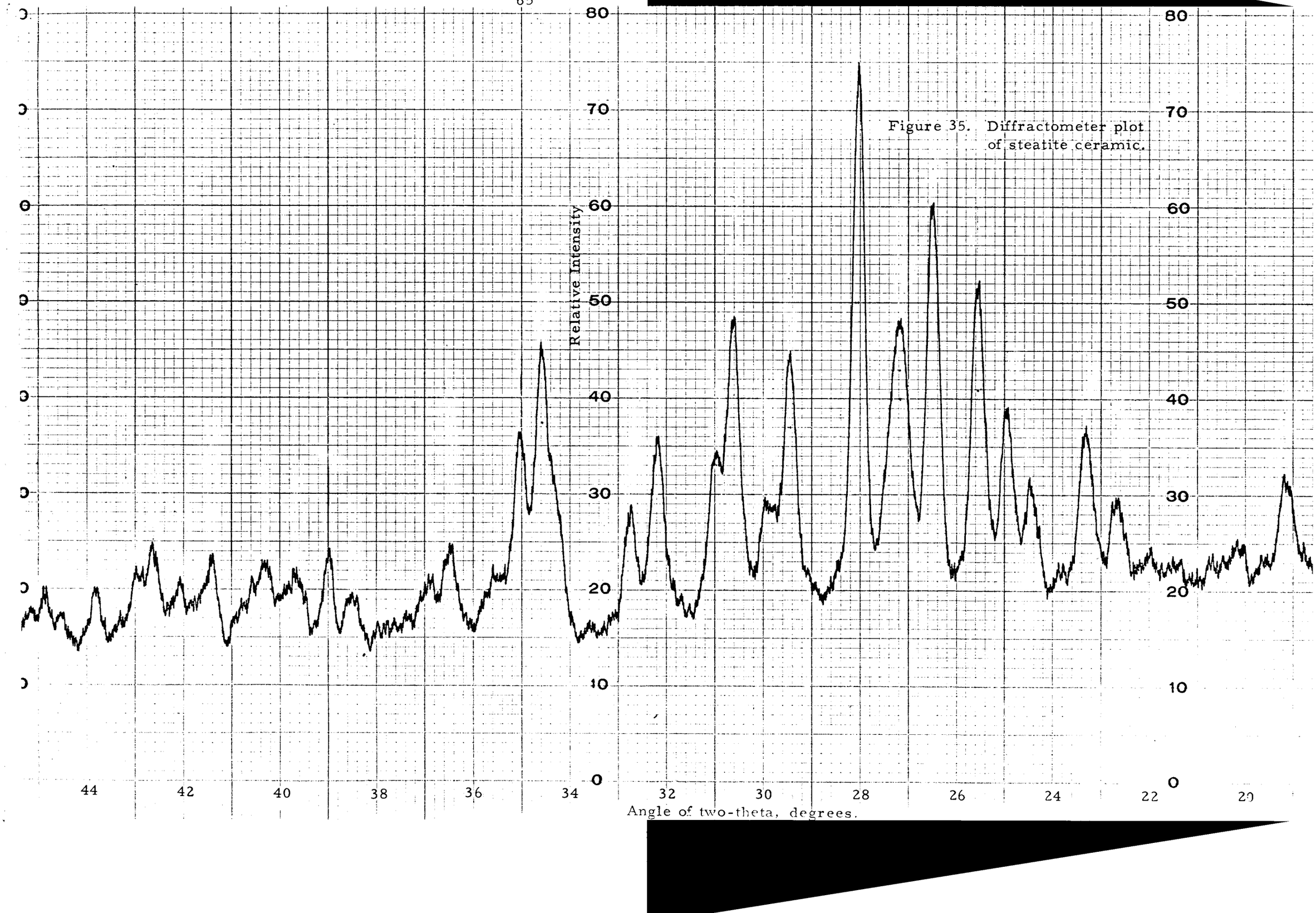

Figure 35. Diffractometer plot of steatite ceramic.

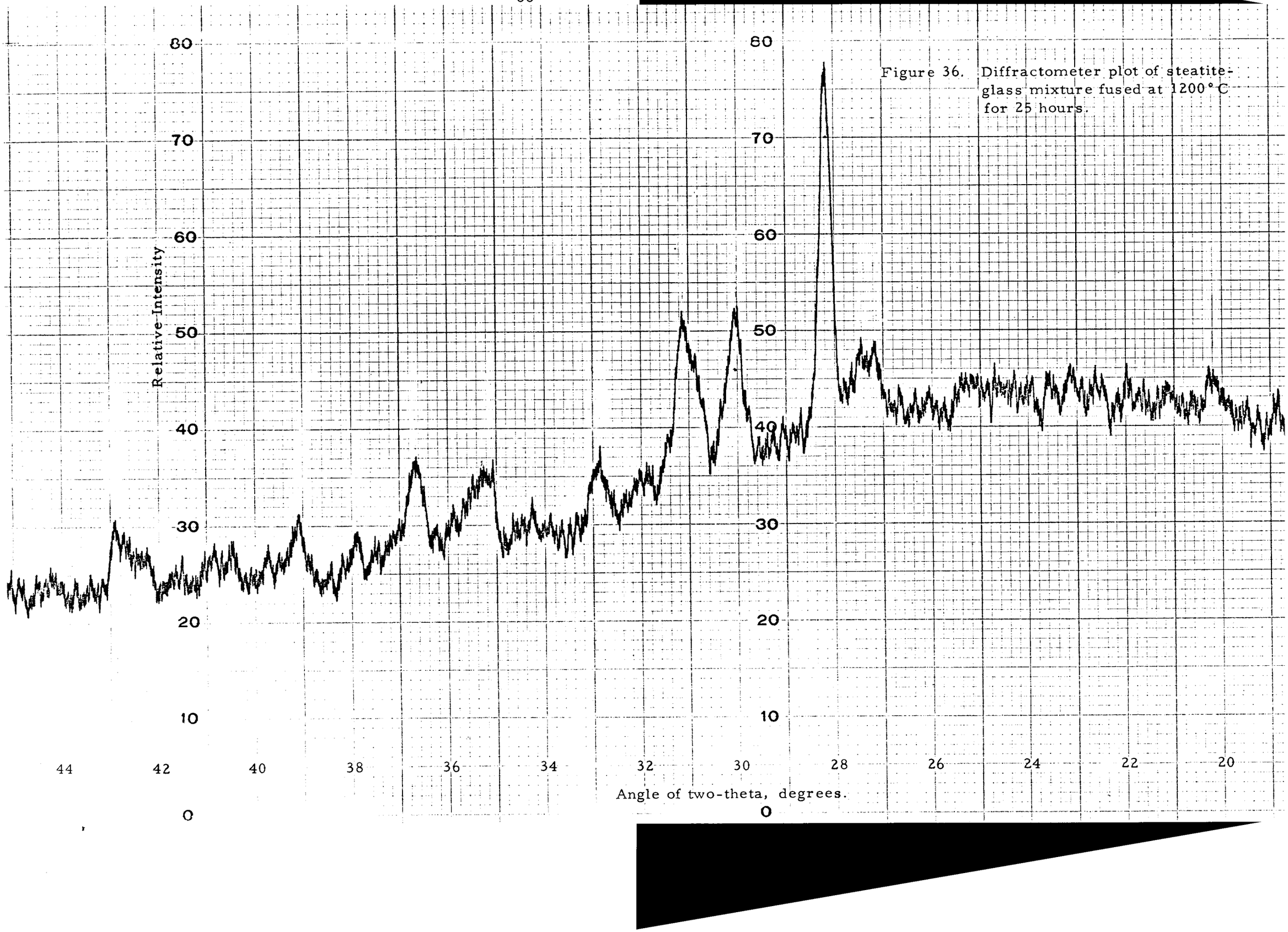

Figure 36. Diffractometer plot of steatite-glass mixture fused at 1200°C for 25 hours.

Table X. Completely randomized analysis of variance of rupture strengths of alumina-7052 seals formed at various temperatures (17).

Treatments	800°	900°	1000°	1100°	1200°	Combination
Obs	0	429	981	-	2125	
in	0	-	1000	970	2720	
lbs.	0	600	1170	2025	2615	
T	0	1029	3151	2995	7460	G = 12,635
n	3	2	3	2	3	$\Sigma n = 13$
$\bar{y}$	0	514.5	1050.3	1497.5	2486.7	$\bar{y} = 1109.8$
$\frac{T^2}{n}$	0	529,420.5	3,309,600.3	4,485,012.5	18,550,533.3	26,874,566.6

Preliminary Calculations

Type of Total	Total of Squares	No. of Items Squared	No. of Obs. Per Sq. Item	Total of Sq. Per Obs.
Grand	G^2	1	13	10,336,401.9
Sample	-	-	-	26,874,566.6
Obs.	-	-	-	27,669,077.0

Analysis of Variance

Source	Sum of Squares	DF	Mean Square	F
Among Sample	16,538,164 7	4	4,134,541.1	41.631
Within Sample	794,510.4	8	99,313.8	
Total	17,332,675.1	12		

Hypothesis: Means of all five treatments are equal.

$$F = \frac{\text{Among Sample Mean Square}}{\text{Within Sample Mean Square}}$$

$(F_8^4)_{obs}$ is 41.631 is greater than $(F_8^4)_{5\%}$ is 3.838.

Therefore, reject hypothesis.

Calculation of Stress in Alumina Seal

Given:

1. Average dimensions of specimen

$$ID = 0.502 \text{ inch}$$

$$OD = 0.750 \text{ inch}$$

$$\text{Ideal Seal Area, } A_s = \frac{\pi}{4}(OD^2 - ID^2) = 0.244 \text{ in.}^2$$

$$\text{Assumed Seal Area, } A_s^a = 2A_s \cong 0.50 \text{ in.}^2$$

2. Dimensions of pressure cylinder

$$ID = 0.502 \text{ inch}$$

3. Approximate force on piston

$$F_p = 2600 \text{ lbs.}$$

4. Force on base of specimen (or seal)

$$F_s = F_p$$ (since area of pressure cylinder equals area on inside of base of specimen)

Calculation of tensile stress on seal

$$\sigma = \frac{F_s}{A_s^a} = \frac{2600 \text{ lbs.}}{0.50 \text{ in.}^2} = 5200 \text{ psi}$$